Comparative study of Ruthenium complexes with organic sensitizer in ZnO based DSSC

By

Muniba Ayub

275109

Session 2018-20

Supervised by

Dr. Nadia Shahzad

MASTER of SCIENCE in

ENERGY SYSTEMS ENGINEERING

US-Pakistan Center for Advanced Studies in Energy (USPCAS-E)

National University of Sciences and Technology (NUST)

H-12, Islamabad 44000, Pakistan

August 2022

Comparative study of Ruthenium complexes with organic sensitizer in ZnO based DSSC

Muniba Ayub

Reg # 00000275109

Session 2018-20

Supervised by

Dr. Nadia Shahzad

A Thesis Submitted to the U.S.-Pakistan Centre for Advanced Studies in Energy in partial fulfillment of the requirements for the degree of MASTER of SCIENCE in ENERGY SYSTEMS ENGINEERING

U.S.-Pakistan Centre for Advanced Studies in Energy (USPCAS-E)

National University of Sciences and Technology (NUST)

H-12, Islamabad 44000, Pakistan

August 2022

THESIS ACCEPTANCE CERTIFICATE

Certified that final copy of MS/MPhil thesis written by Ms. Muniba Ayub, (Registration No. 00000275109), of U.S.-Pakistan Center for Advanced Studies in Energy has been vetted by undersigned, found complete in all respects as per NUST Statues/Regulations, is within the similarity indices limit and is accepted as partial fulfillment for the award of MS/MPhil degree. It is further certified that necessary amendments as pointed out by GEC members of the scholar have also been incorporated in the said thesis.

Signature: _____

Name of Supervisor Dr. Nadia Shahzad

Date: _____

Signature (HoD): _____

Date: _____

Signature (Dean/Principal): _____

Date: _____

Certificate

This is to certify that work in this thesis has been carried out by **Ms. Muniba Ayub** and completed under my supervision in Solar Energy Laboratory, U.S-Pakistan Center for Advanced Studies in Energy, National University of Sciences and Technology, H-12, Islamabad, Pakistan.

Supervisor: _____

Dr. Nadia Shahzad
USPCAS-E
NUST, Islamabad

GEC member # 1: _____

Dr. Zuhair S. Khan
USPCAS-E
NUST, Islamabad

GEC member # 2: _____

Dr. Sehar Shakir
USPCAS-E
NUST, Islamabad

GEC member # 3: _____

Dr. Muhammad Imran Shahzad
National center for Physis
QAU, Islamabad

HoD- (ESE): _____

Dr. Rabia Liaquat
USPCAS-E
NUST, Islamabad

Principal/ Dean: _____

Prof. Dr. Adeel Waqas
USPCAS-E
NUST, Islamabad

Dedication

I dedicate this thesis to my mother because of her support and prayers I wouldn’t be able to complete my research and this degree. She is a hard-working woman who has risen to the challenges in front of her and come out a winner. She is my inspiration, and I would like to be like her someday.

Acknowledgement

I would like to thank my supervisor, Dr. Nadia Shahzad, for her constant support and guidance during my research work. I am also grateful to my GEC members Dr. Zuhair S. Khan, Dr. Sehar Shakir and Dr. Muhammad Imran Shahzad for their valuable feedback and constructive criticism. Most of all I am indebted to my lab fellows and the lab engineers at USPCAS-E, for their help and assistance every step of the way.

Table of Content

Abstract

Ruthenium dyes are a well-known player in the field of DSSCs due to their structure and presence of a novel metal. Their properties and complexes are studied for almost three decades. Although these sensitizers show better performances, their high cost makes these devices less economical. Organic dyes have recently been explored as an alternative to ruthenium-based dyes due to their easy and low-cost synthesis. This is a comparative study between Ruthenium and organic dyes which analysis dicyanoisophorone and Rhodanine organic dyes with ruthenium complexes. The Ruthenium complex named SZD-3 has shown efficiency of 1.208%. High recombination rate at interfaces of photoanode- dye molecule and photoanode- electrolyte molecule degrades the device performance consequently decreasing open-circuit voltages and short circuit current of the device. ZnO metal oxide structure instability in the presence of Ru-dyes is also a player in the lower output of the devices. While organic sensitizers SMA-06 and PT4N are 10-11% efficient as compared to SZD-3.

Keywords: Sensitizers, Ruthenium Complexes, isophorone sensitizer, Rhodanine Sensitizer, DSSC

List of Figures

List of Tables

List of Publications

1. Effect of ZnO nanostructures on the performance of dye sensitized solar cells (Journal: Solar Energy) (Published)
2. Performance analysis of carbon-doped titania (C-TiO2) counter electrode (CE) for dye sensitized solar cells (DSSCs) (Journal: Journal of Materials Science) (Under review)
3. Comparative study of Ruthenium complexes with organic sensitizer in ZnO based Dye-sensitized solar cell (Journal: Bulletin of Materials Sciences (submitted)

Chapter 1

Introduction

1.1 Introduction

Energy is a basic necessity of humans in everyday life for decades and even millenniums. The importance of energy can be seen in the use of several tasks that cannot be done without the use of energy. The energy demands are increasing with time and the advancement of technology. The most important source of energy generation is a fossil fuel that is depleting rapidly, and a very limited amount is left. To conserve these fossil fuels, precautionary measures should be taken to avoid the exhaustion of reserves and alternative resources should be applied for continuous energy supply in the world. Challenges related to energy and its generation are as follow:

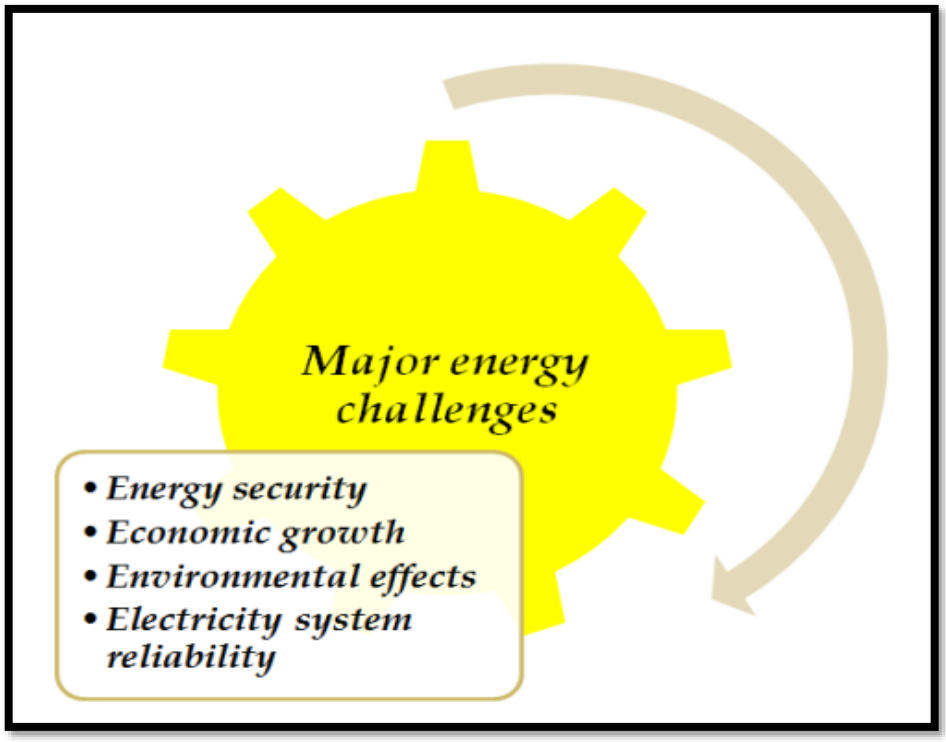

Figure 1.1 Energy Challenges[1]

The consumption and demands of energy are increasing day by day with time and population growth. Furthermore, greenhouse gases (GHG) emissions and environmental

pollution poses a threat to natural habitat and human health. Fossil fuels are the major source of GHG emissions and environmental pollution, but their use is still not limited, and a large amount of energy demands of the world are met by the combustion of fossil fuels. Alternative sources of energy generation are the point of discussion for many countries in order to act in climate emergency. Renewable energy and renewable technologies are the focus of attention as the legislations and policies bound the energy producers to reduce fossil fuel uses, emissions from fossil fuels and their harmful effects[1].

1.2 Renewable Energy Technologies

The renewable technologies to produce clean energy are as follow:

- Wind Energy
- Bioenergy
- Hydropower
- Geothermal
- Tidal energy
- Solar Energy

Energy contributions from renewable technologies are anticipated to increase by $1/5^{th}$ per year to meet the energy demands of the world, from 2018 to 2023. It was forecast that in 2023, 30% of the global energy demand will be met by renewable technologies. In 2017, 24% of global energy demands were met by renewable technologies in which solar technologies were at the top of the energy production list. The second renewable contributor to global energy demands were wind energy followed by hydro and biofuels. Now, 16% share of the world energy production is met by hydropower, 6% form wind energy, 4% from solar energy and 3% from biofuels. It was also anticipated that energy demands for heating and transportation will increase by 10-12%[2].

1.2.1 Wind Energy

The cause of wind is as the earth surface is heated by the sun unevenly, the air adjacent to the surface heated up and flows. It is kind of a solar energy. The sun heats up all the surfaces of earth including oceans, but the oceans are cooler than land at daytime. The air

adjacent to land flows upwards and cooler air from above ocean take its place. This makes the wind[3]. In the energy coming from the sun, only 2% is transferred to wind and about 35% energy is being wasted around 1000 meters. About, 1.26×10^{9}MW of energy is available in the wind that is sufficient to meet global energy demands. Kinetic energy in the wind can be converted into mechanical energy to be utilize in turbine for energy production. Modern wind turbines consist of tree blades and are able to generate several megawatts of energy at high wind speed[4].

1.2.2 Bioenergy

In sustainable development, a constructive role is being played by bioenergy[5]. Bioenergy is the derivative of biomass. Biomass is the main source of bioenergy, which is organic matter formed by photosynthesis in the presence of water and carbon dioxide with sunlight. Solar energy storage medium is chemical energy which can be converted into heat, fuels for transport and electricity. plantation forest, forest residue, industry of crop and timber, animal fats, vegetable oil, industrial organic waste, human settlements and animal husbandry[6][7]. Useful products from biomass can be converted into several ways. Conversion techniques and their development are being considered for the useful energy production for biomass. In electricity generation, cost effective method is cofiring in a coal fired power plant. Commercial dedicated units of biomass combustion in combine heat and power generation (CHP) plants are in operation. Another best suited option for electricity generation is anaerobic digestion which is in use as well. For cleaner, and reliable electricity system, heat and fuel generation of higher quality further improvements are necessary[8].

1.2.3 Hydropower

Moving water produce hydropower. Electricity is generated by conversion of mechanical and kinetic energy of water. It is also a form of solar energy as the hydrologic cycle is driven by the sun, rain is also facilitated by it. Hydrologic cycle makes the atmospheric water reach the surface of earth by rain. Surface run off is the majority of this water as the water percolates in the soil and but some of it evaporates as well. Ponds, lakes, reservoir and ocean are the destination of rain and melting snow which generates electricity with the help of turbine[9]. Many regions of the world relied upon hydro energy which plays an important role in several countries around 150 to generate electricity by hydropower.

It is the largest renewable resource of the world. The commercial electricity in ten countries such as Norway, Bhutan, Paraguay, and several African countries comes from hydro. About 19% of global energy production which accounts for 2600 TWh/year is expected to be operational globally making hydro power about 700 GW[10].

1.2.4 Geothermal

Earth's heat or geothermal energy is a sustainable and clean resource of energy. It has been used for centuries for bathing, washing, health and cooking. It is one of the most adaptable energy sources. As the new applications arises, the geothermal energy is utilized in direct hot water uses and increasing rapidly. About 24 countries were using electricity from geothermal energy in late 2013 and about 78 countries using heating from geothermal energy. The growth of geothermal energy is increasing day by day which has reached about 10.7 GWe in total installed capacity of geothermal[11]. Somegeothermal energy uses rely on the earth's temperatures near the surface, while others necessitate drilling kilometers below the ground. The earth's temperature near surface is sometimes utilized in geothermal but most of the time kilometers below the ground, drilling has been done for it. Applications of geothermal energy are as follow [12]:

- **Direct Use:** Spring and reservoir in the vicinity is utilized for the hot water needs.
- **Power generation:** Water and steam temperature ranging from 300 to 700degree Fahrenheit is the requirement of a power plant. Mostly, the geothermal reservoir is near the power plant is in the range of 2 miles.
- **Geothermal heat pumps:** Temperature of the buildings are controlled by geothermal heat pumps by utilizing water temperature near earth's surface

1.2.5 Tidal Energy

Research and development stage of tidal energy is not done, and it is not commercialized yet. It is a new renewable technology that is not yet economically feasible. Tidal energy is limitless sources of energy. The main advantage of this energy is that it is not subjected to climate change as other renewable energies, as climate changes does not affect it[13]. It is estimated theoretically that tidal energy that can be harvested near the coast locations is about 1 terawatt (TW), globally. In

comparison, Tidal current technologies are more advantageous than Tidal range technologies. About 514 MW total tidal range was present in 2012. It was estimated that about 200 MW for tidal current will be developed till 2020. The best part of tidal energy is that it is not intermittent, and energy can be generated at night or day. Neither it is being affected by weather conditions and changes. It provides several alternatives for power generation[14].

- At ebb tide, power generation one way
- At flood tide power generation one way
- Power generation two way.

1.2.6 Solar Energy

Among renewable energy resources, Solar energy is a well-known source of energy. Solar energy can be used in ways such as electrically, chemically, and thermally. Although solar energy is abundant, and it is practically available almost everywhere, but only small amount of solar energy is utilized. In the worlds output of electricity, solar energy only accounts for 0.015%. For global space and water heating, solar energy contributes about 0.3%. The most common use of solar energy is in the form of biomass, its natural process production, gasification, and combustion. Photocatalysis is used in solar energy for the use of hydrogen production. About 11% of energy demands of humans are fulfilled by hydrogen production[15].

1.3 Harvesting Technologies

Solar Energy can be harvested by three techniques [15].

1. Solar Fuel
2. Solar Thermal
3. Electricity

1.3.1 Solar Fuel

Splitting of water using solar energy is a cleaner, greener, and sustainable alternative for future as it can reduce global warming. Hydrogen production is mainly done by water splitting that requires high temperatures or voltages to separate oxygen and

hydrogen molecules in water. As the photosynthesis which utilizes sunlight and produces chemical energy solar hydrogen production also utilizes photon energy conversion into chemical energy. Researchers are focusing to produce an artificial photosynthesis devices such as “artificial leaf” that will be helpful in capturing, converting and storing solar energy as chemical fuel[15].

1.3.2 Solar Thermal

Heating requirements can be fulfilled by suing solar energy in the form of drying, heating, and cooling at industries and residences. For low temperature requirements, Solar flat plate collector is used. For high temperature applications, concentrated solar collectors are utilized. Solar energy is also applied for wastewater and saline water treatments to save the environment.[15][16].

1.3.3 Electricity

Electricity generation is further divided into two categories [17].

- PV Technologies
- Solar Thermal Power generation

1.3.3.1 Solar Thermal Power Generation

Concentrated solar collectors are used to generate electricity. Steam is formed from water at a point where mirrors magnify and concentrated solar energy. Frensel, power towers and solar dish are used in solar concentrated energy and high temperature application. Arrays of reflecting mirrors in quantity of thousand are utilized for power[17] [16].

1.3.3.2 PV Technologies

In PV, semiconductors are used. The sunlight produces electricity after conversion the semiconductors. The electron of semiconductors travels across the bandgap of it by absorbing a photon which creates an electron hole pair and P-n junction. The changes move in opposite directions which is responsible for the creation of potential difference[15].

1.3.3.2.1 Classification of Solar PV Cells

Classification of Solar PV depends upon the times they were introduced and the materials that are being used in it[18]. There are four generations of solar cells.

1.3.3.2.1.1 First Generation

The silicon based solar cells are first generation solar cells. These are of two types: mono and poly crystalline solar cells. The material waste that is produce in the manufacturing of first generation of solar cells is high and that's makes the first-generation solar cells expensive and less environmentally friendly.

1.3.3.2.1.2 Second Generation

To overcome the drawback of first-generation solar cells, second generation solar cells were introduced. These cells are nanoscale thin films that reduces the cost and wastage of material being used. Silicon in amorphous form, cadmium zinc tin sulfide (CZTS), cadmium telluride, and cadmium indium gallium selenide (CIGS).

1.3.3.2.1.3 Third Generation

Third generation solar cells used organic and inorganic materials for light management in the device. These cells are dye-sensitized solar cells, perovskite solar cells, photo chemical cells and quantum dot cells.

1.4 Dye Sensitized Solar Cells

In comparison to silicon based solar cells, DSSC became a better alternative. It has several advantages such as easy fabrication, chape, flexible and transparent. The commercialization of DSSC can become easy because of all these advantages. In 1991, Gratzel and O'Regan first introduced DSSC at UC Berkeley[19], hence also known as Gratzel cells. The first DSSC consists of TiO_2 nanoparticles as semiconductor film and dye layer coating on it for charge transfer.

1.4.1 Component of DSSCs

A DSSC is made by joining different components together. A photoanode which is a working electrode is the main component of a DSSC. The dye which is a sensitizer is sensitized on the photoanode is used as absorbance and performance enhancer. A counter electrode which is usually platinum electrode deposited on an FTO. An electrolyte is present between two electrodes that are sandwiched together, which is a redox mediator which provide charges to oxidized sensitizers[20].

1.4.2 Working of DSSCs

A glass or plastic conductive substrate is used for the deposition of working electrode and counter electrode. The substrate act as a contact which collects charges. The substrates are usually transparent above 80% to be able to pass the sunlight effectively towards the active area of the cell in order to get high efficiency. To reduce the energy losses from the substrate and better charge transfer kinetics, electrical conductivity of the substrate should be high. Here are some of the characteristics of substrate:

1) Flourine doped Tin Oxide (FTO, SnO_2: F)

   Transmittance ~ 75%

   Sheet Resistance ~ 8.5 Ω cm^{-2}

2) Indium doped Tin Oxide (ITO, In_2O_3: Sn)

   Transmittance ~ 80%

   Sheet Resistance ~ 18 Ω cm^{-2} [21]

The photoanode which is also called working electrode is prepared by semiconductor oxide nanolayer or micro layer on the surface of a substrate either glass or plastic. The semiconductors oxides are usually ZnO, TiO_2, and Nb_2O_5. These materials are the best options for this layer because of their wider band gap between 3-3.2 eV. The titanium dioxide is usually the preferred choice because of low cost and non-toxicity. The problem with these materials is that only a small region of UV light is absorbed by these so sensitizations of dyes are done on the surface of metal oxide layers. The sensitized dye on the metal oxide surface attach itself by covalent bonding with the metal oxide. It is suggested to have a highly porous layer of metal oxide on the photoanode to have more dye adsorbed on it which can harvest more sunlight. For the sun light to be absorbed on the surface of photoanode, dyes play an important role. The days that can absorb light in the range from UV visible to near infra-red are desired dyes. These are luminescent dyes. It is desired that the highest occupied molecularorbital (HOMO) of dye molecule should be higher than conduction band of metal oxide. Likewise, and lowest unoccupied molecular orbital (LUMO) of dye molecule should be higher than

conduction band of semiconductor metal oxide material. It is also suggested that the compatibility of electrolyte with the dye orbital are very important. The main role of electrolyte is charge transport and dye regeneration. The most commonly used electrolytes are Co(II)/Co(III) [22], I^-/I^{-3},Br^-/Br^{-2}[23] and SCN^-/SCN_2 [24]. For an ideal electrolyte, it should be able to regenerate the dye oxidize molecules and should remain stable electrochemically and thermally inside the DSSCs for longer period of times. In the previously state electrolytes, Iodine electrolyte has been used extensively because of the reported good results[25] the only drawback with iodine electrolyte is degrades the device as it corrodes the electrodes, contributes in dye desorption and makes the device less stable[26]. For the photoanode conduction band enhancement which enhances the open circuit voltage, TBP (4-Tert-butylpyridine) is used to avoid charge recombination on the surface of titanium dioxide from electrolyte used[27]. The light strikes a DSSC device and the electrochemical changes in it generates power which produces electricity. It is also called artificial photosynthesis because the process is similar to actual photosynthesis. The dye is the real working element in a DSSC as the light absorbs on the surface of the DSSC and the dye molecules gets excited and jump from ground state which is HOMO (highest occupied molecular orbital to excited state which is LUMO (lowest unoccupied molecular orbital) and the electron that is emitting is called photogenerated electron. Semiconductor metallic oxide photoanode is n-type material that electron conductor as well as electron acceptor[28]. The electron of dye which gets excited by light transfer from dye to conduction band of photoanode semiconductor metallic oxide material[19]. Because of this, hole and electron pair generates as an electron transfers from dye to metal oxide surface leaving a hole behind and dye in its oxide state[29]. Energy different for this excited state LUMO and ground state HOMO can be given buy following equation of enthalpy[30].

$$\Delta h = \Delta E = E_{LUMO} - E_{HOMO} \quad (1.1)$$

here,

Δh = enthalpy Change

ΔE = energy Change

E_{LUMO} = LUMO energy

E_{HOMO} = HOMO energy

The electron that came to the metal oxide surface from dye is transported to the conductive substrate and produces current by flowing through an external circuit[31]. The electricity is generated through this, and the speed of this process is very fast. The hole appears in the dye because of loss of electron is filled by electrolyte which regenerate dye by giving electron. The electron deficiency of the electrolyte is filled by the electron coming from the counter electrode which is receiving electron form the external circuit[16]. Working principle of DSSC is shown in Figure 2.

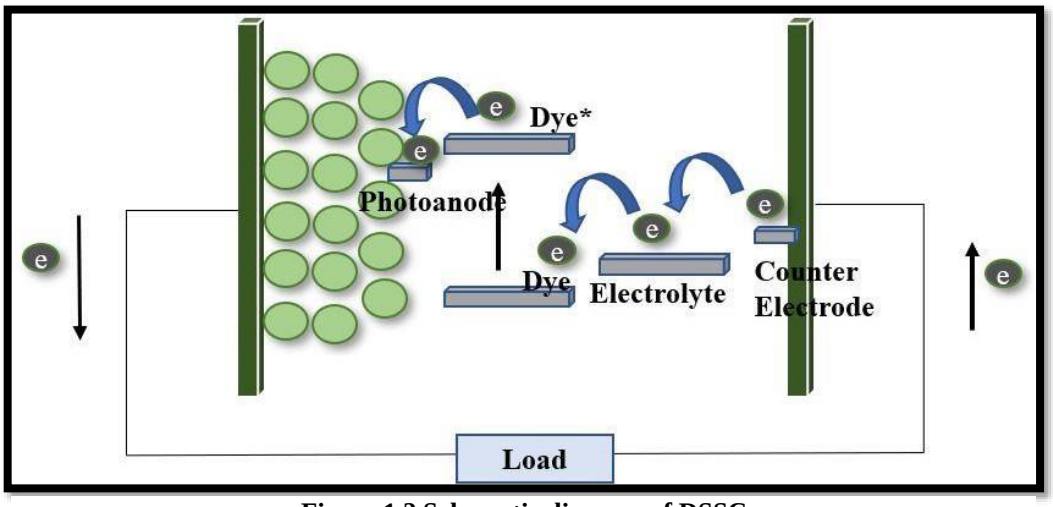

Figure 1.2 Schematic diagram of DSSC

Different factors define the efficiency of DSSC. Energy levels of different components and charge transfer kinetics are the well-known factors to define DSSC efficiency.

1.4.3 Applications of DSSCs

There is no vacuum required for the fabrication of DSSCs and it can easily be fabricated in open environment which reduced its cost of production[32]. This lower cost of manufacturing makes these a sustainable alternative for commercialization in future. When these are compared with silicon based DSSCs, its production cost account for 1/5 to 1/10[33]. Different colors in dyes can be used for aesthetic appeal inside the vicinity such as windows and sunroofs[34]. DSSCs can also be flexible and easily fabricated by synthesizing photoelectric materials for conversion. At higher air mass, DSSC module shows enhanced efficiencies because of Voc and Jsc degradation[35]. In building integrated PV (BIPV) better efficiency and performance is shown by transparent

DSSC[36]. Plastic substrate gives a better alternative for light weight DSSC production, and it can be used in several applications related to light weight DSSC. This will rise as a new brand market[34].

1.5 Pakistan's Status of Renewable Energy

According to yearly report of NEPRA 2020, power generation capacity of Pakistan is 38700 MW in which 31 % of energy is coming from Hydro and 4 % is coming from renewable energy including wind, solar and Bagasse. AEDB (Alternate Energy Development Board) is monitoring 22 solar projects with the capacity of 890 MW, from which 6 solar projects are working and generating about 400 MW solar energy. Remaining 16 projects are at different stages of completion [37]

1.6 Problem Statement

Ruthenium complexes are a well-known player in the fabrication of a DSSC. Complicated synthesis and expensive material requirements make them less attractive and feasible for the fabrication of DSSC and its economics. This is a limitation and problem for the development of the DSSCs.

1.7 Research Objectives

The Objectives of this research are:

- ✓ Examine the performance of Ruthenium dyes in DSSC
- ✓ Examine the performance of rhodamine and dicyanoisophorone organic dye in DSSC
- ✓ study the interaction of ZnO photoanode with ruthenium complexes
- ✓ study the interaction of ZnO photoanode with rhodamine and dicyanoisophorone Organic dyes
- ✓ Conclude the properties and drawbacks in ruthenium, rhodamine and dicyanoisophorone dyes in ZnO based DSSC

Chapter Summary

For energy demands of current period of time, use of renewable energy is better than conventional energy uses. Solar energy as an alternative can generate electricity and heat. Different type of solar technologies and cells can be used for the generation of electricity. Solar cells can be categorized into three generations depending upon their advancement and technology. Silicon based solar cells are the first-generation solar cells that is commercialized technology being used in institutes, industries, homes, and hospitals for electricity generation. But this technology is expensive, and the production cost and steps require huge amount of heat and expenses. In contrary, third generation DSSC are cheap and simple fabrication of these make them more environmentally friendly.

References

[1] H. Balcioglu and K. Soyer, “Renewable Energy– Background,” no. November, 2017, doi: 10.6084/m9.figshare.6169460.

[2] I. - International Energy Agency, “Market Report Series: Renewables 2018.”

[3] “Wind Power-Energy from Moving Air.”

[4] W. Tong, “CHAPTER 1 Fundamentals of wind energy,” *WIT Trans. State Art Sci. Eng.*, vol. 44, pp. 1755–8336, 2010.

[5] Visa, “Annual Report 2017,” *NTT Docomo*, vol. 21, no. 5, p. 430, 2017.

[6] “(PDF) Chapter 1: Biomass and Bioenergy.” [Online]. Available: https://www.researchgate.net/publication/309127353_Chapter_1_Biomass_and_Bioenergy. [Accessed: 24-Nov-2021].

[7] U. Rasool and S. Hemalatha, “A review on bioenergy and biofuels: sources and their production,” *Brazilian J. Biol. Sci.*, vol. 3, no. 5, p. 3, 2016.

[8] S. Schuck, “Bioenergy in Australia - Status and opportunities,” *5th Asia-Pacific Conf. Combust. ASPACC 2005 Celebr. Prof. Bob Bilger’s 70th Birthd.*, pp. 41–46, 2005.

[9] “Hydropower Program | Bureau of Reclamation.” [Online]. Available: https://www.usbr.gov/power/. [Accessed: 24-Nov-2021].

[10] “(PDF) Hydroelectric Power.” [Online]. Available: https://www.researchgate.net/publication/315493188_Hydroelectric_Power. [Accessed: 24-Nov-2021].

[11] H. Saibi, S. Finsterle, R. Bertani, and J. Nishijima, “Geothermal energy,” *Handb. Sustain. Eng.*, pp. 1019–1042, Jan. 2013.

[12] “Geothermal explained - U.S. Energy Information Administration (EIA).” [Online]. Available: https://www.eia.gov/energyexplained/geothermal/. [Accessed: 07-Dec-2021].

[13] "(PDF) Tidal Energy: A Review." [Online]. Available: https://www.researchgate.net/publication/310795127_Tidal_Energy_A_Review. [Accessed: 25-Nov-2021].

[14] I. Renewable Energy Agency, "Tidal Energy Technology Brief," 2014.

[15] G. Crabtree, N. L.-A. C. Proceedings, and undefined 2008, "Solar energy conversion," *aip.scitation.org*, vol. 1044, p. 309, 2008.

[16] N. Kannan and D. Vakeesan, "Solar energy for future world: - A review," *Renew. Sustain. Energy Rev.*, vol. 62, pp. 1092–1105, Sep. 2016.

[17] E. Kabir, P. Kumar, S. Kumar, A. A. Adelodun, and K. H. Kim, "Solar energy: Potential and future prospects," *Renew. Sustain. Energy Rev.*, vol. 82, pp. 894–900, 2018.

[18] "Solar Cell - an overview | ScienceDirect Topics." .

[19] B. O'Regan and M. Grätzel, "A low-cost, high-efficiency solar cell based on dye-sensitized colloidal TiO2 films," *Nat. 1991 3536346*, vol. 353, no. 6346, pp. 737–740, Oct. 1991.

[20] K. Sharma, V. Sharma, and S. S. Sharma, "Dye-Sensitized Solar Cells: Fundamentals and Current Status," *Nanoscale Res. Lett. 2018 131*, vol. 13, no. 1, pp. 1–46, Nov. 2018.

[21] U. Mehmood, S. U. Rahman, K. Harrabi, I. A. Hussein, and B. V. S. Reddy, "Recent advances in dye sensitized solar cells," *Adv. Mater. Sci. Eng.*, vol. 2014, 2014.

[22] H. Nusbaumer, J. E. Moser, S. M. Zakeeruddin, M. K. Nazeeruddin, and M. Grätzel, "CoII(dbbip)22+ Complex Rivals Tri-iodide/Iodide Redox Mediator in Dye-Sensitized Photovoltaic Cells," *J. Phys. Chem. B*, vol. 105, no. 43, pp. 10461–10464, Nov. 2001.

[23] S. Ferrere, A. Zaban, and B. A. Gregg, "Dye Sensitization of Nanocrystalline Tin Oxide by Perylene Derivatives," *J. Phys. Chem. B*, vol. 101, no. 23, pp. 4490–4493, Jun. 1997.

[24] G. Oskam, B. V. Bergeron, G. J. Meyer, and P. C. Searson, “Pseudohalogens for dye-sensitized TiO2 photoelectrochemical cells,” *J. Phys. Chem. B*, vol. 105, no. 29, pp. 6867–6873, Jul. 2001.

[25] F. Gao *et al.*, “Enhance the optical absorptivity of nanocrystalline TiO2 film with high molar extinction coefficient ruthenium sensitizers for high performance dye-sensitized solar cells,” *J. Am. Chem. Soc.*, vol. 130, no. 32, pp. 10720–10728, Aug. 2008.

[26] J. Wu *et al.*, “Progress on the electrolytes for dye-sensitized solar cells,” *Pure Appl. Chem.*, vol. 80, no. 11, pp. 2241–2258, Jan. 2008, doi: 10.1351/PAC200880112241/MACHINEREADABLECITATION/RIS.

[27] A. Kay and M. Grätzel, “Low cost photovoltaic modules based on dye sensitized nanocrystalline titanium dioxide and carbon powder,” *Sol. Energy Mater. Sol. Cells*, vol. 44, no. 1, pp. 99–117, Oct. 1996.

[28] M. K. Nazeeruddin, E. Baranoff, and M. Grätzel, “Dye-sensitized solar cells: A brief overview,” *Sol. Energy*, vol. 85, no. 6, pp. 1172–1178, Jun. 2011.

[29] M. Grätzel, “Dye-sensitized solar cells,” *J. Photochem. Photobiol. C Photochem. Rev.*, vol. 4, no. 2, pp. 145–153, Oct. 2003.

[30] J. Bisquert, D. Cahen, G. Hodes, S. Rühle, and A. Zaban, “Physical Chemical Principles of Photovoltaic Conversion with Nanoparticulate, Mesoporous Dye-Sensitized Solar Cells,” *J. Phys. Chem. B*, vol. 108, no. 24, pp. 8106–8118, Jun. 2004.

[31] D. Wei, “Dye Sensitized Solar Cells,” *Int. J. Mol. Sci. 2010, Vol. 11, Pages 1103-1113*, vol. 11, no. 3, pp. 1103–1113, Mar. 2010.

[32] S. Sathyajothi, R. Jayavel, and A. C. Dhanemozhi, “The Fabrication of Natural Dye Sensitized Solar Cell (Dssc) based on TiO2 Using Henna And Beetroot Dye Extracts,” *Mater. Today Proc.*, vol. 4, no. 2, pp. 668–676, Jan. 2017.

[33] “(PDF) Materials for Enhanced Dye-sensitized Solar Cell Performance: Electrochemical Application.” [Online]. Available:

https://www.researchgate.net/publication/272943912_Materials_for_Enhanced_Dye-sensitized_Solar_Cell_Performance_Electrochemical_Application. [Accessed: 07-Dec-2021].

[34] J. Gong, J. Liang, and K. Sumathy, “Review on dye-sensitized solar cells (DSSCs): Fundamental concepts and novel materials,” *Renew. Sustain. Energy Rev.*, vol. 16, no. 8, pp. 5848–5860, Oct. 2012.

[35] “(PDF) Application of Dye-Sensitized Solar Cell Technology in the Tropics: Effects of Air Mass on Device Performance.” [Online]. Available: https://www.researchgate.net/publication/261614314_Application_of_Dye-Sensitized_Solar_Cell_Technology_in_the_Tropics_Effects_of_Air_Mass_on_Device_Performance. [Accessed: 07-Dec-2021].

[36] S. Yoon, S. Tak, J. Kim, Y. Jun, K. Kang, and J. Park, “Application of transparent dye-sensitized solar cells to building integrated photovoltaic systems,” *Build. Environ.*, vol. 46, no. 10, pp. 1899–1904, Oct. 2011.

[37] “Pakistan - Renewable Energy.” [Online]. Available: https://www.trade.gov/country-commercial-guides/pakistan-renewable-energy.

Chapter 2

Literature Review

2.1 Introduction

This chapter will discuss different type of sensitizers used in dye sensitized solar cells. Ruthenium dyes and their complexes, different type of organic dyes, their properties and draw backs will be briefly explained.

2.2 Characteristics of Dyes

The progress that has been reported in the dye optimization has been done by metal, ligands and metal and transition metal complexes by candidate of substitute groups. The development of mononuclear and polynuclear dye is made by systematic study of metals i.e., Re, Pt, Os, Cu, Fe and Ru. A variety of organic molecules have been tested, some of those are squaraine, indoline, hemicyanine, coumarin and donor acceptor organic dyes. The highest efficiency that is reported by these dyes is 8%. Some research has also been done on phthalocyanine and porphyrin dyes. There are some design requirements a dye need to have just to function properly inside a DSSC. There should be a proper anchoring group present which binds the dye molecules with the surface of metal oxide surface. Strong bonding of dye molecule to photoanode surface are necessary efficient electron transfer from the dye to metal oxide surface and for electrolyte leaching prevention. Some of the anchoring groups are phosphonic acid and carboxylic. The excited state of the dye should be high so that the electron transfer to semiconductor metal oxide become easy. Likewise, the ground state of dye molecule should be low enough so that regeneration of oxidized dye molecules is not difficult from electrolyte. An ideal dye should be able to absorb sunlight in the region of visible and near IR spectrum of sunlight. It should be able to transfer photogenerated electron rapidly to the metal oxide surface as compared to going back to its ground state. It is recommended to use dyes showing emission at room temperature but it is not necessary[1].

2.3 Ruthenium Dyes

It is noted that the Ruthenium complexes consists of Ruthenium metal as center atom and ligands such as tetrapyridine or bipyridine and NCS as auxiliary ligand. These dyes show charge separation. Structures of Ru complexes such as N3, N719 and N749 are presented in Figure. 2.1. The first Ru complex that has been first developed was N3 in 1991 which is (RuL_2X_2) complex. It has two dipyridyl ligands and two X ligands (NCS). Two N electron are given by dipyridyl molecules, and one N donor electron is given by NCS ligand. There are other ruthenium dyes that are developed after the development of N3 by the Gratzel group.

The reason for the popularity of Ru dyes is that these dyes show good photoelectric properties. These dyes also have energy band structure that helps in the maximum absorption of light and shows maximum absorption. To improve the efficiency of a dye it is suggested to increase the electron lifetime in LUMO and absorbance of visible region light. There are studies that make changes in the structure of Ru dye to achieve the above requirements by changing the X ligand of the complex that only donates one electron. When N3 was in the development phase, the X ligand choice was made by analyzing different ligands such as Br, Cl, I, CN, NCS and H_2O and NCS was selected because of its ability of MLCT which made the development of N3 possible. It is reported that N3 dye gives results about 80-85% IPCE but the absorbance of light by N3 is limited and cannot absorbance longer wavelength photons of visible region (η of 10 %).

To increase the absorbance of N3, a new dye was developed which is black dye. In the structure of black dye, one monoprotonated hydrogen is present on the polypyridyl ligand that can be adsorbed on the photoanode. This was done to reduce the dye aggregation on the surface of metal oxide photoanode and decrease intermolecular hydrogen bonding. This dye can absorbance light even in the near infrared region showing efficiency of 10.4 %. The reason for larger wavelength light absorption is due to MLCT red shift. Although the molar extinction coefficient of black dye is lower than N3 and the adsorption on the surface of photoanode is also small, the black dyes PCE has been shown improved results. Among all the Ru based Complexes, N719 has been reported the best efficiency so far. The molecules similar to N719 having carboxylic acids, when adsorbed on the surface of metal oxide, it loses its hydrogen. This makes the surface of the photoanode positive, and

the fermi level decreases. This helps in the adsorption of the dye molecules on the surface of photoanode material and the transfer of charge from the LUMO of dye after light absorption to the metal oxide photoanode. Although some aspects of the dyes enhance by the number of hydrogens increase in the structure such as photocurrent but the open circuit voltages and overall conversion decreases because of the changes of fermi level of metal oxide and electrolyte. These results gave an idea for the development of a new dye N719 which shows highest efficiency of 11.18% in Ruthenium complexes[2].

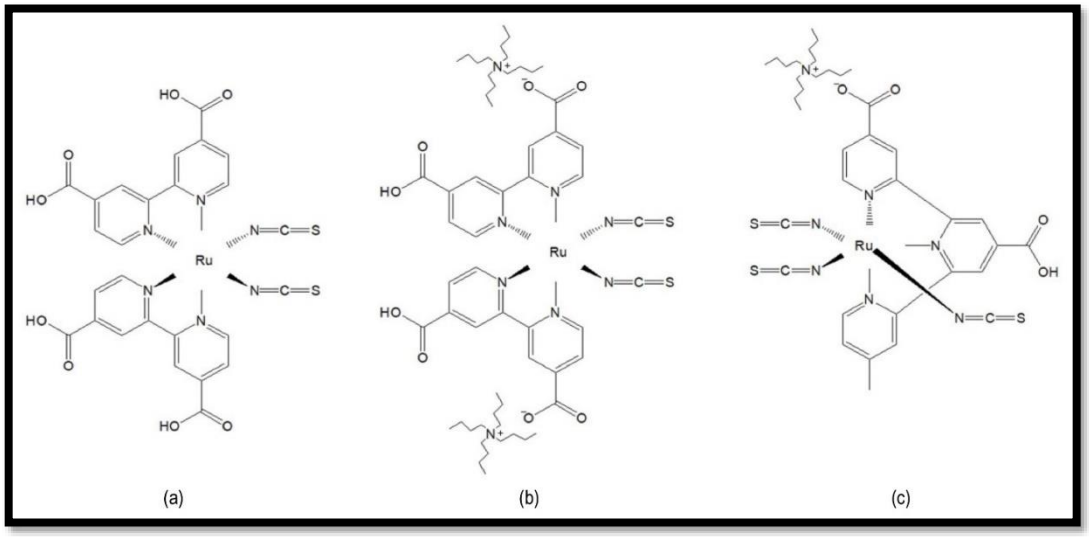

Figure 2.3 Structure of Ruthenium Dyes (a) N719 (b)N3 (c)N749[2]

The styryl group has shown promising results. Two new ruthenium complexes S1 and S2 are developed in which former has a pyrrole extended ligand and later one has a styryl group. These two dyes containing pyrrole has various reason to be interested in. The electron donating effect is brought by bipyridine ligand which has a pyrrole pound by nitrogen. This results in the energy level rise of the ground states of the dye which allows the MLCT transition at the lower energy and absorption of light with the red shift. In addition to that, molar extinction coefficient can also be increased by pyrrole π-electron. An extended absorption in S2 compared to N3 dye is because of the π-delocalization. S1 dye is giving better performance with the redox mediator Co $(DTB)_3^{2+}$/$Co(DTB)_3^{3+}$ couple (DTB = 4,4′-diterbutyl-2,2′-bipyridine) (IPCE 62%) and S2 performed better with I^-/I_3^- couple (IPCE 75%). These dyes can also be used in the solid-state devices as the presence of pyrrole make it possible to be polymerize. It is also noted that the NCS influence the behavior of dyes and both of the NCS ligands behave differently. One of the

NCS groups favors in charge transfer and second one draw electron density from another anchoring group carboxylic group COOH which discourage the charge transfer. The MLCT and LLCT both can be found in the UV region of the light. The ligand choice can be used in the development of a favorable dye design and structural tunning[3].

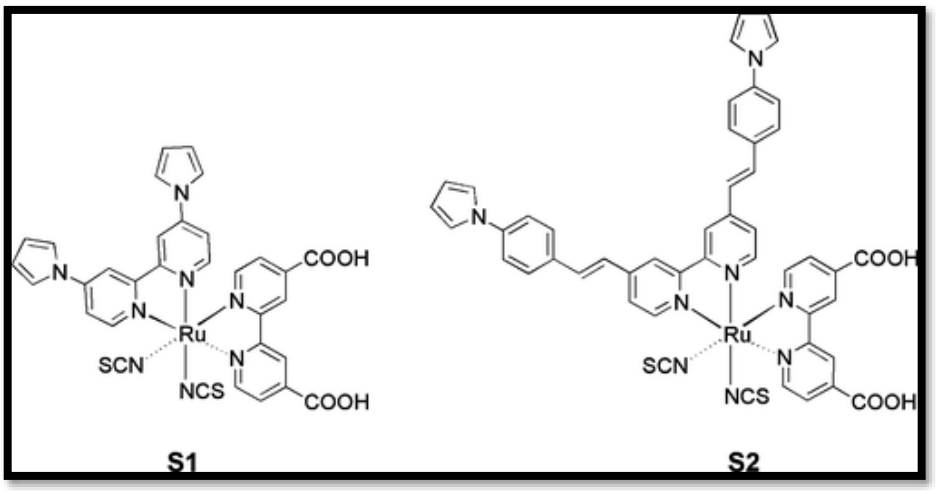

Figure 2.4 Structure of S1 and S2 dye[3]

Figure 2.3 is showing CYC-B6S and CYC-B6L dyes structure. CYC-B6S has shown better performance than CYC-B6L as opposing the same energy level orbital structures and absorption region. It clearly indicates that the absorption and energy levels of a dye cannot define its performance parameters as well as the size and the amount of dye adsorbed on the surface of metal oxide surface also are responsible for the performance on the dye[4].

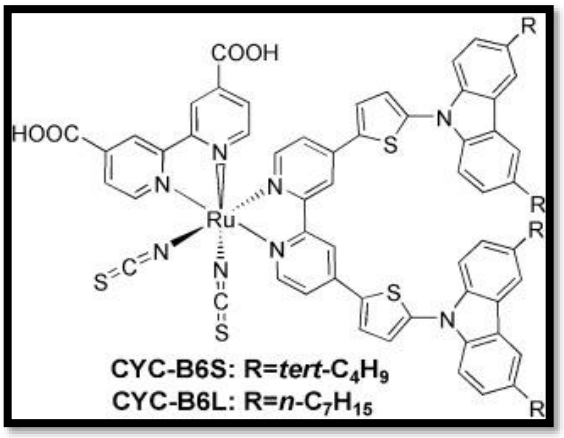

Figure 2.5 Structure of CYC-B6S and CYC-B6L[4]

An efficiency of 3.42% has been reported by the presence of ligand (E)-5-nitro-N1-(pyridin-4-ylmethylene) benzene-1,2-diamine (NPD-PC) on the structure of the dye along with the Voc of 0.79 V, Jsc of 7.12 mA/cm^2 and FF of 0.61. This efficiency is the result of the dual anchoring group in the structure of the dyes which indicates that the more the number of anchoring groups in the structure of dye, the better the binding of dye on the surface of the metal oxide as compared to less anchoring groups. One of the reasons which hinders the commercialization of DSSC is its stability for longer periods of time. It is reported that the RNPDA has proved to be stable for 80h while producing efficiency[5]

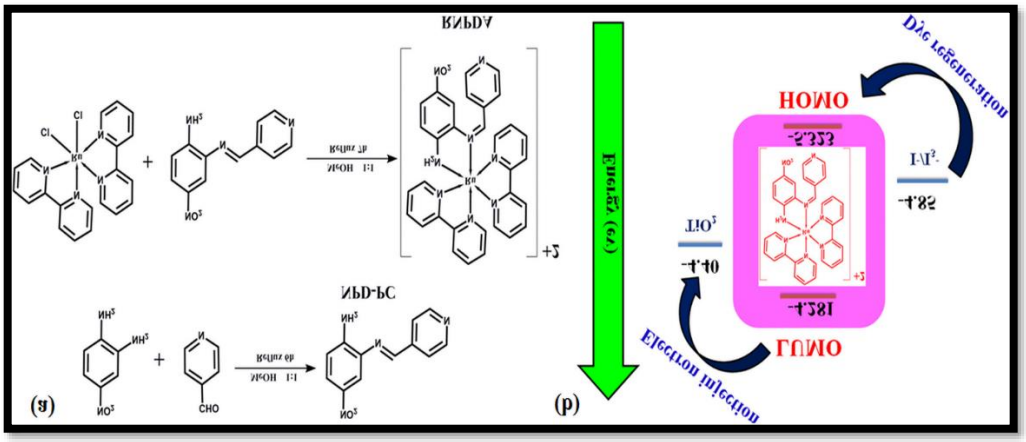

Figure 2.6 Synthesis and Energy diagram of RNDPC[5]

As presented in Figure. 2.5. Ru-D1 and Ru-D2 dyes are analyzed in DSSC. These two dyes were tested against a Reference cell made of N719. The Voc reported by the cell sensitized by these dyes have reported 0.74 V as compared to 0.60 V of the reference cell. It is reported that Ru-D1 has shown 23% Voc betterment as compared to the refence N719 cell. This makes these dyes a suitable candidate for the use in a DSSC application. These dyes have shown lower FF and photocurrent because of the higher recombination rate. The Ru-D1 has reported efficiency of 1.46% while Ru-D1 has shown 1.13% efficiency[6].

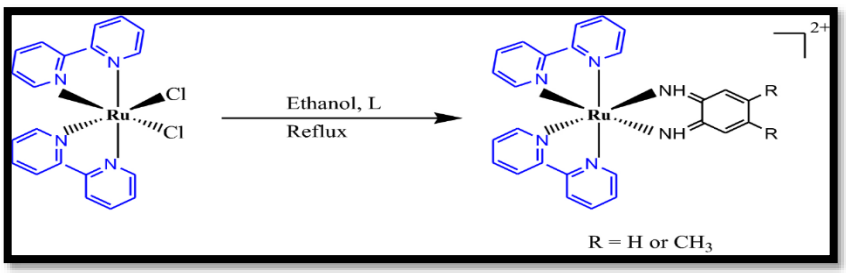

Figure 2.7 Structure of Ru-D1 and Ru-D2[6]

A new Ru senstizer was developed by the replacement of dcbpy ligands in N3 dye by abtpy, which is a bipyridine ligand substituted with alkyl bithiophene groups and the Sensitizer is named as CYC-B1. The structure of CYC-B1 is presented in the Figure. 2.6. This sensitizer has shown the efficiency of 8.54% in the DSSC which is about 10% higher than N3 dye with the same conditions and parameters for fabrication. It has also shown the Voc and Jsc values that are closer to the N3 dyes reported values. The reason for higher efficiency of this dye is because of the higher Jsc values coming from the MLCT of dcbpy higher absorption coefficient. On the surface of metal oxide, water induced desorption of dye molecules have been prevented by alkyl group on the abtpy ancillary ligand. It is also suggested that this dye can give better stability in the DSSC[7].

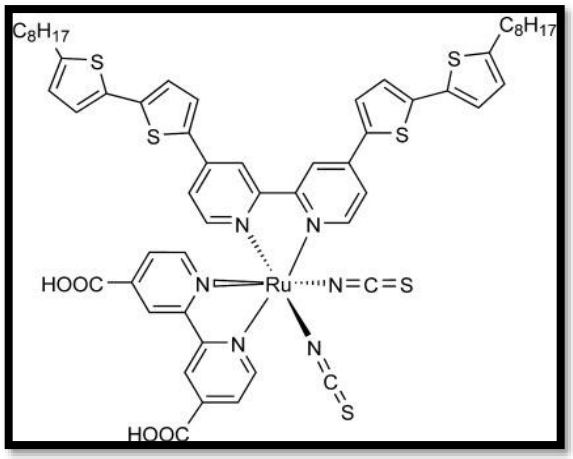

Figure 2.8 Structure of CYC-B1[7]

A new Ru-complex having ancillary ligand of hexasulfanyl–styryl-modified bipyridyl group has been developed. The structure of this Ru-polypyridine sensitizer (TGA) is shown in the Figure. 2.7. This sensitizer has a high absorption coefficient and small red shift absorption. This higher absorption coefficient of TGA is responsible for better sensitization of the metal oxide thin films on the photoanode. TGA has also proved better performance as compared to N719 as it has reported 11.4 mA of photocurrent in comparison with N719 which has only reported 9.0 mA. In the device fabricated by using TGA, the electrolyte that was used promotes electron injection high quantum efficiency but have lower voltages for both dyes. It is also revealed that TGA can perform better than N719 in the same condition, but it needs some structural modification before achieving

highest efficiency than N719. The only draw back of the TGA is the electrode/electrolyte recombination, which is because of the p- system extension[8].

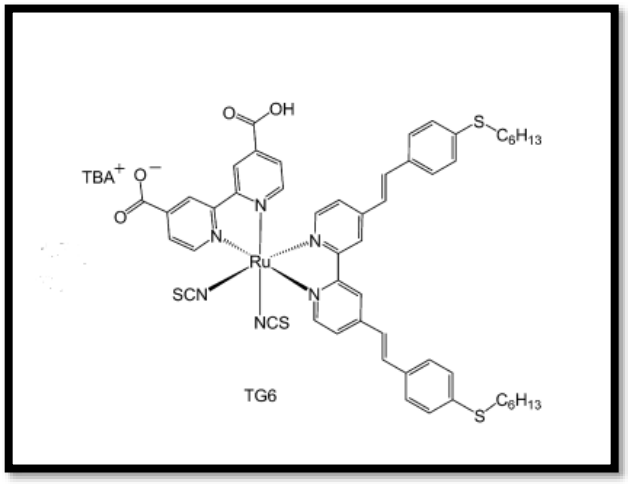

Figure 2.9 Structure of TGA[8]

Ru sensitizers, CBTR and CfBTR are shown in the Figure. 2.8. These sensitizers have reported higher Voc values such as 730 and 710 mV, respectively as compared to N719 which has only reported 700mV under the same conditions. This is because these sensitizers influence the fermi level of the metal oxide surface in the same way as N719 while binding to the surface of the metal oxide. CBTR has reported efficiency of 9.69% which is about *% higher than N719 efficiency of 8.98% under the same conditions and fabrications. This higher efficiey of CBTR is because of the NHC ligand which donate a strong σ electron resulting in the higher Jsc value. The CfBTR has only shown slightest elevated efficiency than N719 which was 9.04% It is suggested that the enhanced efficiency of CBTR can also efficiently donate electron to the metal oxide conduction band after photo excitation of the electron. It is revealed that the molecular tuning of Ru sensitizers can results into higher efficiencies of DSSC and the presence of NHC–pyridine group can be a promising candidate in the structure of Ru sensitizers. It clearly depicts that the these sensitizers can used in the DSSC and give better results[9].

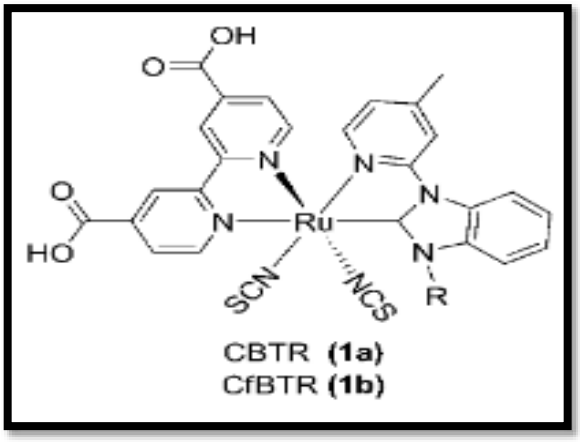

Figure 2.10 Structure of CBTR and CfBTR[9]

New sensitizers in the family of Ru complexes have been developed in the class of cyclometallated ruthenium (II) complexes, (Ru(tctpy)(C^N)(NCS) (**1**, **2**). In the structure of this sensitizer, bidentate cyclometallating ligand which is a C^N is used indicating 2-phenylpyridinato or 2-(4-(2-phenylethynyl) phenyl) pyridinato. The structure of these senitizers is shown in Figure.2.9. It is reported that the sensitizer 2 has higher IPCE values as compared to sensitizer 1. This higher efficiency of 2 is because of the higher molar extinction coefficient of dye 2 which is also responsible for the extended absorption of light up to near IR region. The output parameters of sensitizer 1 and 2 are as follow: Isc: 6.1 mA cm^{-2} and 9.1 mA cm^{-2} , Voc: 0.53 V and 0.58 V, FF: 0.69 and 0.70 and efficiency: 2.2% and 3.7%, respectively. It is also noted that the efficiency and performance of these dyes can further improved by optimization of the devices and the structural modification of C^N ligand in the sensitizers[10].

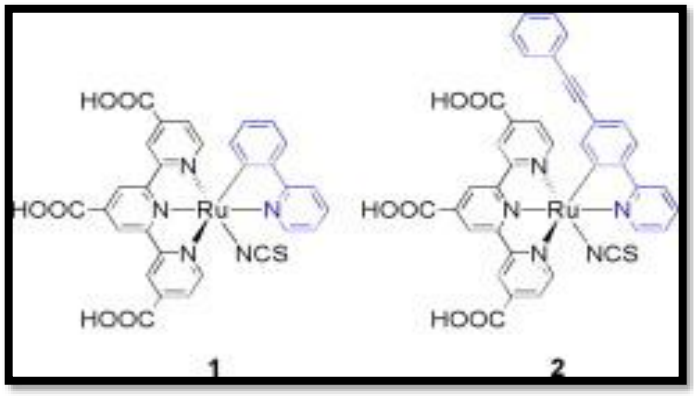

Figure 2.11 Structure of Ruthenium dye 1 and 2[10]

2.4 Organic dyes

A lot of research has been done on the development of organic sensitizers. This is because organic sensitizers have a number of advantages on inorganic sensitizers which are easy preparation and purification method with low costs, they can harvest more wavelength of light in the visible and IR region, have high molar extinction coefficient and a variety of structural modification which can help the in the use of desired substituting groups that can be responsible for better photo physical and electrochemical results in the application in the DSSC. These dyes have vast number of resources as there is no limitation of material as no rare element is used in the preparation of organic dyes. Many organic dyes have reported high performances in DSSC which were structurally designed and developed for the application of DSSC[11].

Four organic sensitizers NKX-2553, NKX-2554, NKX-2569, and NKX-2600 which are shown in the Figure. 2.10, are developed. These conjugated novel organic dyes having electron donor moieties of *N*, *N*-dimethylaniline (DMA) and electron acceptor moieties of cyanoacetic acid (CAA) were used in the DSSC. These dyes have shown good performance in the DSSC. The dye NKX-2569 has shown the highest efficiency of 6.8% under irradiation of 1.5 AM, with Voc of 0.71V, Jsc of 12.9 mA cm±2 and FF of 0.74. the improved performance of the dyes is because of the smooth electron injection of dye to the conduction band of metal oxide surface. It is noted that the use of organic sensitizers in the DSSC will not only lower the cost of DSSC production but also provide higher performance of the DSSC[12].

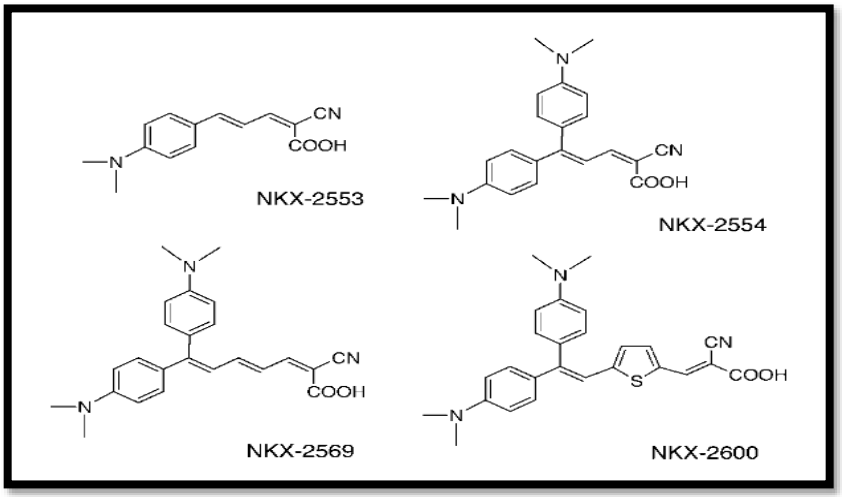

Figure 2.12 Structure of Novel Conjugated dye[12]

A series of dyes named as DS-1, DS-2, DS-3, and DS-4 presented in Figure.2.11, are developed for the application of DSSC. These series of sensitizers have D−π−A scheme. The photovoltaic results of DS-1, DS-2, and DS-4 are higher than DS-3, which has only shown 5.12% of overall efficiency. The sensitizer DS-2 has given 7.00% overall efficiency with the Voc of 633 mV, Jsc of 15.3 mA/cm^2 and FF of 72.5. This efficiency is better than the reported triphenylamine-based DSSCs which has previously only reported efficiencies are between 2.47-6.15%. The sensitizers DS-1 and DS-4 has shown efficiency of 6.71% and 6.57%, respectively. It is revealed that the Electron spacer in the structure of dyes influences the overall efficiencies and performance of the dyes in the DSSC. The DS-2 dye has shown better result in comparison to DS-1 because of the inclusion of another single bond thiophene unit. The Jsc of DS-2 was slightly higher than DS-1 device. Thienothiophene electron spacer in the structure of DS-4 has reduced the efficiency of the dye as the dye aggregation on the surface of metal oxide is promoted by it. It is understood that a single layer on the surface of metal oxide is required for efficient charge transfer of photoexcited electron to the conduction band of metal oxide. The dye molecules aggregation on the surface of metal oxide is responsible for electron recombination resulting in the decrease of Voc value as the Voc output of DS-4 was 610mV. The DS-3 has shown the lowest results in the series of dyes although the absorption of the light by this dye was extended. The presence of vinyl unit in the spacer from (E)-1,2-bis(5-formyl-2-thienyl) ethane) is responsible for the complicated intramolecular charge transfer in the excited state resulting in the lower excited energy and electron injection efficiency as reported earlier. The vinyl unit is also responsible for the Voc decrease which leads to the dye aggregation on the surface of metal oxide[13].

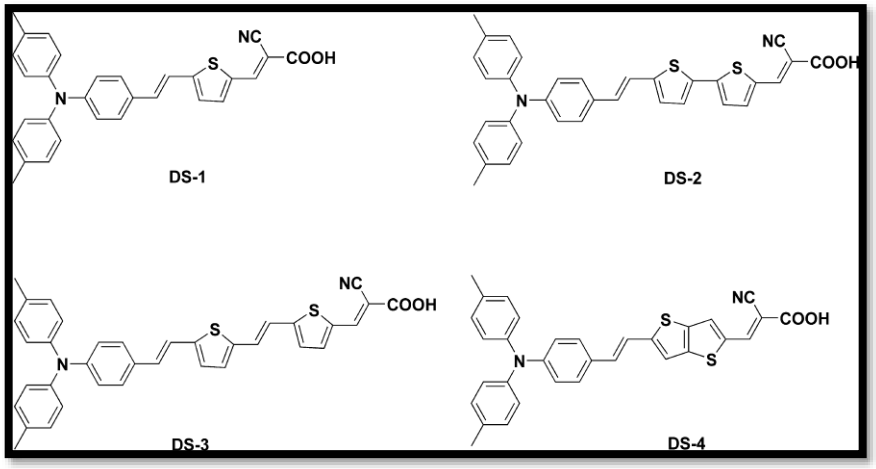

Figure 2.13 Structure of organic dye DS-1, DS-2, DS-3 and DS-4[13]

A water-soluble organic sensitizer represented in the Figure. 2.12 was developed and named as Eosin Y. The dye has pink color and show fluorescence in yellow green. This dye is already used in several fields as it is used in fluorescent pigment, printing and dyeing as well. The Isc of the device fabricated by the sensitization of eosin Y on the photoanode is1.020 mA/cm^2. The Voc is 0.671 V and the FF ranged from 42.4% to 59.6%. The highest efficiency achieved by the Eosin Y is 0.399% in the fabricated DSSC[14].

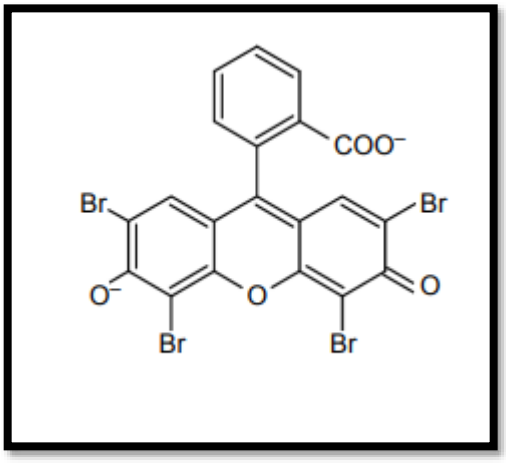

Figure 2.14 Structure of Eosin Y organic dye[14]

A sensitizer named SSD1 which is represented in the Figure. 2.13, having chromophores with donor/accepter capability in a spiro configuration was developed to be used in DSSC. This dye has shown similar behavior in DSSC as the devices fabricated by using N3 dyes. This sensitizer is efficient in keeping the positive charge away from the metal oxide surface resulting in the better performance of the dye. This behavior reduces charge

recombination as the back transfer of electron is reduced. The two carboxylate anchoring groups provides the bivalent binding of the dye molecule on the surface of metal oxide and reduces charge recombination as the metal oxide surface is separated from photogenerated electron donating molecules. The output parameters of the cells fabricated by the dye are: Jsc = 8.9 mA cm^{-2}, Voc = 0.63 V, FF = 0.67 and efficiency of 3.75%[15].

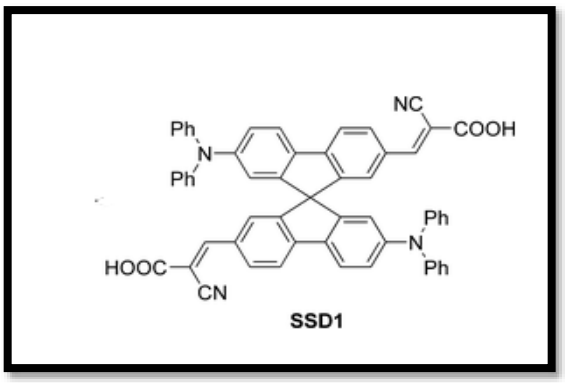

Figure 2.15 Structure of SSD1 organic dye[15]

Two novel organic sensitizers named as DRA-BDC and DTB-BDC presented in Figure. 2.14. are developed. These sensitizers contain electron acceptors in the form of rhodanine-3-acetic acid/thiobarbituric acid and electron donors and spacers in the form of N, N-butyl dicarbazole to be used in DSSC. The DSSC output of DRA-BDC and DTB-BDC are 0.92 and 0.59 V od Voc, respectively. These values shows that these sensitizers efficiently inject electrons from LUMO of dyes to conduction band of meta oxide films. These dyes efficiency can be calculated by the variation of energy between excited state of dye to conduction band of metal oxide film. The theoretical efficiency of these devices is 1.29 and 0.73 eV/PCBM. These values reveal that electron junction of dyes by these sensitizers are powerful[16].

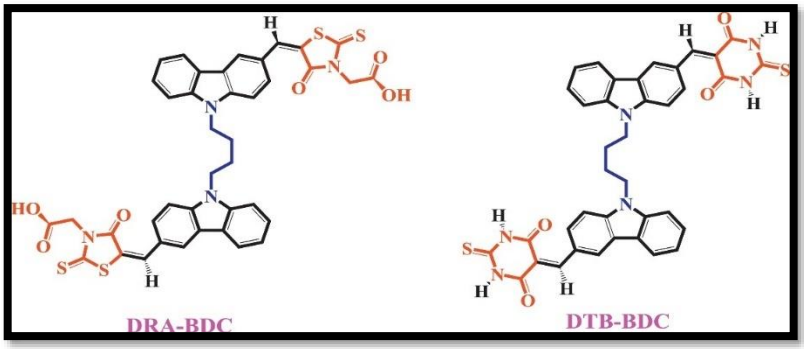

Figure 2.16 Structure of Dye DRA-BDC and DTB-BDC[16]

Three new organic sensitizers named L0, L1 and L2 are represented in Figure. 2.15, were synthesis. These sensitizers having donor moiety of a triphenylamine, acceptor of a rhodanine-3-acetic acid and a connection of polyene. These donor and acceptors are linked by methine and thiophene moieties. The red shift response of these dyes and the reduced positive oxidized potential is because of the conjugated length increased in the dyes. The device was fabricated using titanium dioxide as photoanode sensitized by these dyes and iodide/triiodide electrolyte. The lowest efficiency among the dyes is shown by L2, due to lower charge collection and dye regeneration. A photocurrent reduction is also observed by the addition of 4-tert-butylpyridine in the electrolyte which decreases the electron injection efficiency. A negative shift in the conduction band of thin film was observed of 0.15 V[17].

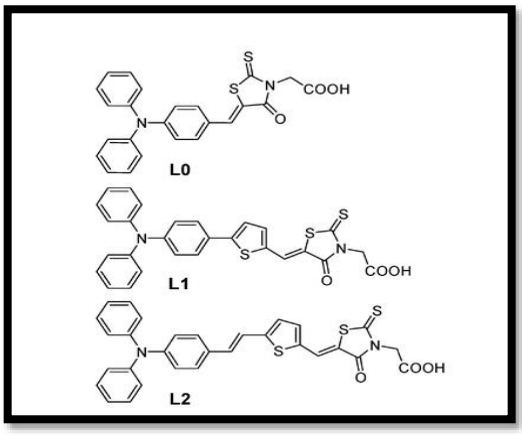

Figure 2.17 Structure of L0, L1 and L2[17]

An organic sensitizer series of R1, R2 and R3 are represented in Figure. 2.16, are formed to be used in DSSC. These sensitizers contain electron donating moieties of carbazole, iminodibenzyl, and phenothiazine, electron accepting and anchoring moiety of rhodanine ring. The device output prepared by using R1, R2 and R3 dye is Voc of 587 mV, 625 mV and 661 mV, Jsc of 6.62 mA/cm ^{2}, 7.46 mA/cm^2 and 10.34 mA/cm^2 and overall efficiency of 2,54%, 3.52%, and 4.87%, respectively under same conditions. The highest efficiency of R3 has shown because of phenothiazine ability to donate electron from donating moiety to accepting moiety. The higher value of Voc is also contributing to the overall enhanced efficiency of phenothiazine substituted dyes[18].

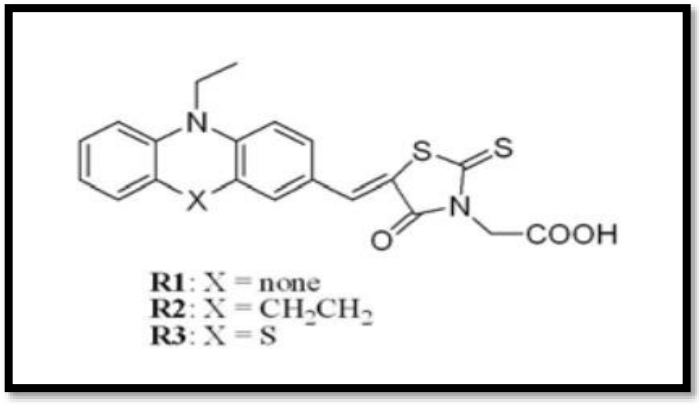

Figure 2.18 Structure of Dye R1, R2 and R3[18]

The synthesis of hemicyanine and Dicyanoisophorone was done to prepare dyes to be used in DSSC. These dyes contain D-π-A strategy. The anchoring group present in the dyes are carboxylic (COOH) acid. The efficiency of SLN-01 is reported to be 0.13% as compared to reference cell which was prepared by the use of N719 having efficiency of 1.58% on ZnO based DSSC. It is noted that DCI dyes are better alternative for ZnO based DSSCs than Cyanine dyes[19].

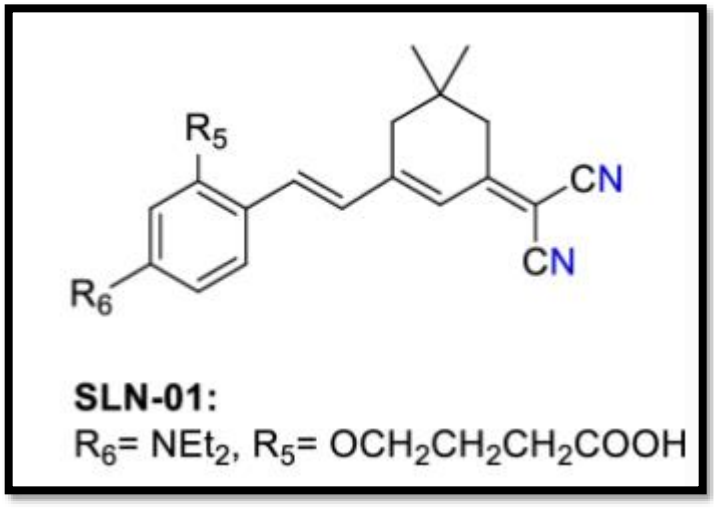

Figure 2.19 Structure of Dye SLN-01[19]

In this work, Ruthenium complexes are being used as sensitizers in the ZnO-based DSSC. Ruthenium complexes are a well-known player in the study and fabrication of DSSCs. Ru Complexes used in this study contains unique nitro, amine, and carboxylic anchoring groups along with thiocyanate. The carboxyl group as ligand promotes an increase in molar extinction coefficient, smooth attachment of dye molecule on semiconductor

surface and secure close coupling between conduction band of semiconductor and excited state wave function of dye molecule[3]. Ambidentate nature of thiocyanate makes it able to attach with a metal either with nitrogen or sulfur. Thiocyanate isomer of N-bound is efficient in solar cell. The N-bound thiocyanate facilitate charge transfer from electrolyte by interacting with ligand at sulfur end which increases the efficiency of dye sensitized solar cell. Nitro, amine, and carboxylic acids anchoring groups have been used in the Ruthenium complexes previously, but their incorporation in a single molecule is new in these complexes. The absorbance of these complexes solutions has shown appreciative results.

The organic sensitizers used in this study are Rhodanine and dicyanoisophorones. Dicyanoisophorone used in named as SMA-06. The absorbance of SMA-06 solution has shown comparative results with Rhodanine sensitizer. Rhodanine sensitizer used in this study is PT4N, which has also shown appreciative absorbance.

Chapter Summary

This chapter describes literature review of different type of Ruthenium complexes and Organic dyes with their photovoltaic performances in DSSCs. The structure and output parameters of dyes used in DSSCs are presented along with the factors attributing to the final outcome of the DSSCs. Organic dyes are better alternative in comparison with Ruthenium complexes because of their cost-effective synthesis with comparable results.

References

[1] N. Robertson, "Optimizing Dyes for Dye-Sensitized Solar Cells," *Angew. Chemie Int. Ed.*, vol. 45, no. 15, pp. 2338–2345, Apr. 2006.

[2] S.-H. Nam, K. H. Lee, J.-H. Yu, and and J.-H. Boo, "Review of the Development of Dyes for Dye-Sensitized Solar Cells," *Appl. Sci. Converg. Technol.*, vol. 28, no. 6, pp. 194–206, Nov. 2019.

[3] A. Monari, X. Assfeld, M. Beley, and P. C. Gros, "Theoretical study of new ruthenium-based dyes for dye-sensitized solar cells," *J. Phys. Chem. A*, vol. 115, no. 15, pp. 3596–3603, Apr. 2011.

[4] C.-Y. Chen *et al.*, "Multifunctionalized Ruthenium-Based Supersensitizers for Highly Efficient Dye-Sensitized Solar Cells," *Angew. Chemie*, vol. 120, no. 38, pp. 7452–7455, Sep. 2008.

[5] K. Subramaniam, A. B. Athanas, and S. Kalaiyar, "Dual anchored Ruthenium(II) sensitizer containing 4-Nitro-phenylenediamine Schiff base ligand for dye sensitized solar cell application," *Inorg. Chem. Commun.*, vol. 104, pp. 88–92, Jun. 2019.

[6] A. S. A. Almalki *et al.*, "Enhancement of the open-circuit voltage of the dye-sensitized solar cells using a modified ruthenium dye," *Appl. Phys. A Mater. Sci. Process.*, vol. 127, no. 3, pp. 1–8, Mar. 2021.

[7] C.-Y. Chen, S.-J. Wu, C.-G. Wu, J.-G. Chen, and K.-C. Ho, "A Ruthenium Complex with Superhigh Light-Harvesting Capacity for Dye-Sensitized Solar Cells," *Angew. Chemie*, vol. 118, no. 35, pp. 5954–5957, Sep. 2006.

[8] F. Matar, T. H. Ghaddar, K. Walley, T. DosSantos, J. R. Durrant, and B. O'Regan, "A new ruthenium polypyridyl dye, TG6, whose performance in dye-sensitized solar cells is surprisingly close to that of N719, the 'dye to beat' for 17 years," *J. Mater. Chem.*, vol. 18, no. 36, pp. 4246–4253, 2008.

[9] W.-C. Chang *et al.*, "Highly Efficient N-Heterocyclic Carbene/Pyridine-Based Ruthenium Sensitizers: Complexes for Dye-Sensitized Solar Cells," *Angew. Chemie*, vol. 122, no. 44, pp. 8337–8340, Oct. 2010.

[10] T. Funaki *et al.*, "Synthesis of a new class of cyclometallated ruthenium(II) complexes and their application in dye-sensitized solar cells," *Inorg. Chem.*

Commun., vol. 12, no. 9, pp. 842–845, Sep. 2009.

[11] Y. Ooyama and Y. Harima, "Molecular Designs and Syntheses of Organic Dyes for Dye-Sensitized Solar Cells," *European J. Org. Chem.*, vol. 2009, no. 18, pp. 2903–2934, Jun. 2009.

[12] K. Hara *et al.*, "Novel Conjugated Organic Dyes for Efficient Dye-Sensitized Solar Cells**,".

[13] G. Li, K.-J. Jiang, Y.-F. Li, S.-L. Li, and L.-M. Yang, "Efficient Structural Modification of Triphenylamine-Based Organic Dyes for Dye-Sensitized Solar Cells,".

[14] T. M. El-Agez, S. A. Taya, K. S. Elrefi, and M. S. Abdel-Latif, "Dye-sensitized solar cells using some organic dyes as photosensitizers," *Opt. Appl.*, vol. XLIV, no. 2, 2014.

[15] D. Heredia *et al.*, "Spirobifluorene-bridged donor/acceptor dye for organic dye-sensitized solar cells," *Org. Lett.*, vol. 12, no. 1, pp. 12–15, Jan. 2010.

[16] M. S. Abusaif *et al.*, "New carbazole-based organic dyes with different acceptors for dye-sensitized solar cells: Synthesis, characterization, dssc fabrications and density functional theory studies," *J. Mol. Struct.*, vol. 1225, p. 129297, Feb. 2021.

[17] T. Marinado *et al.*, "Rhodanine dyes for dye -sensitized solar cells : spectroscopy , energy levels and photovoltaic performance," *Phys. Chem. Chem. Phys.*, vol. 11, no. 1, pp. 133–141, Dec. 2008.

[18] T. Y. Wu *et al.*, "Iranian Chemical Society Synthesis and Characterization of Three Organic Dyes with Various Donors and Rhodanine Ring Acceptor for Use in Dye-Sensitized Solar Cells," 2010.

[19] G. Shabir *et al.*, "The Development of Highly Fluorescent Hemicyanine and Dicyanoisophorone Dyes for Applications in Dye-Sensitized Solar Cells," *J. Fluoresc.*, vol. 32, no. 2, pp. 799–815, Mar. 2022.

Chapter 3

Experimental and Characterization Techniques

3.1 Introduction

Experimental are conducted for the fabrication of a DSSC. These experiments are preparation of Photoanode and counter electrode by using doctor blade, sensitization of photoanode by sensitizers and Fabrication of cell. Characterization, dyes, photoanode and cell is carried out in every step in between the experimentation procedures. Techniques used for the experimentation will be listed here:

3.2 Experimental Techniques

Experimentation techniques to fabricate a dye sensitized solar cell with their working principle will be discussed here:

3.2.1 Deposition Techniques for electrodes fabrication

For the preparation of photoanode or working electrode and counter electrode of a DSSC several techniques are used. Simply, a conductive thin film is deposited on the surface of a substrate in order to prepare a photo and counter electrode. This deposition of conductive material can be done by any of the available techniques of deposition. In this chapter some of these techniques will be discussed in detail.

3.2.1.1 Solution based Synthesis

Some of the Solution based techniques for the deposition of conductive material on the surface of DSSC will be discussed below.

3.2.1.1.1 Doctor Blading

This is the simplest and low-cost method to deposit a thin film on the surface of a glass or plastic substate. This is also called tape casting method. It is usually used when large surface area is deposited by thin films materials because of the ease of procedure and

simplicity. For doctor blading two techniques are used. Rectangular frame doctor blading and spiral film application technique

i) Rectangular Frame Doctor Blade

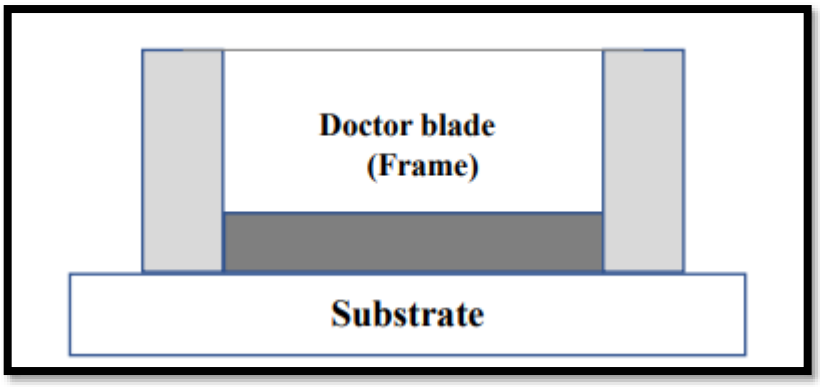

Figure 3.20 Doctor blade principle, frame reservoir moving over the substrate[1]

A reservoir is used in the method of this technique. Literature has already reported the sol flow behavior from the reservoir geometry[2]. Two situations can be adopted while using this method. In one condition, the doctor blade can be used a stationary form and the surface that need to be casted is movable for material layer deposition Fig 3.1. redrawn from literature [1], which depicts the doctor blading technique. To control the thickness of the deposited material, substrate and doctor blade gap is adjusted which is represented in Figure 3.2.

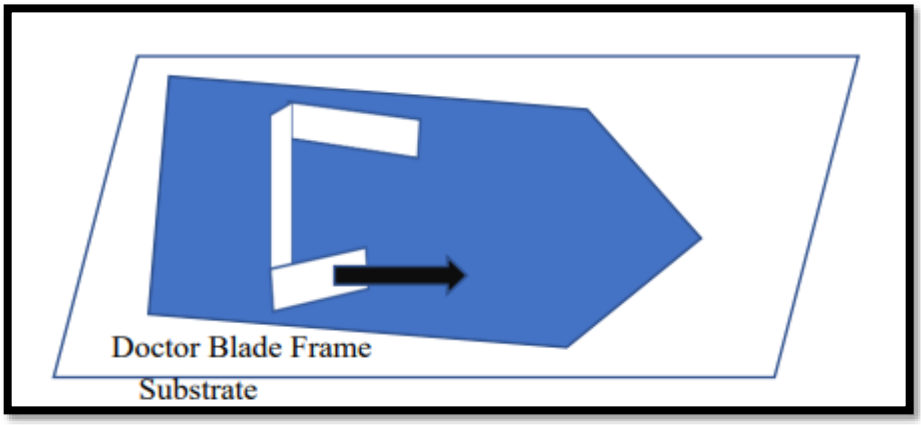

Figure 3.21 Thickness of layer control by gap between doctor blade and frame[1]

Literature has also reported more than on blade use at a time for different applications [3]. Dual blades are also responsible for the accurate, controlled, and precise thickness

of the depositing layer. Plastic foils can also be coated by liquids using doctor blade[4]. As shown Figure. 3.3, the web beneath the blade moves and doctor blade is position with a roller.

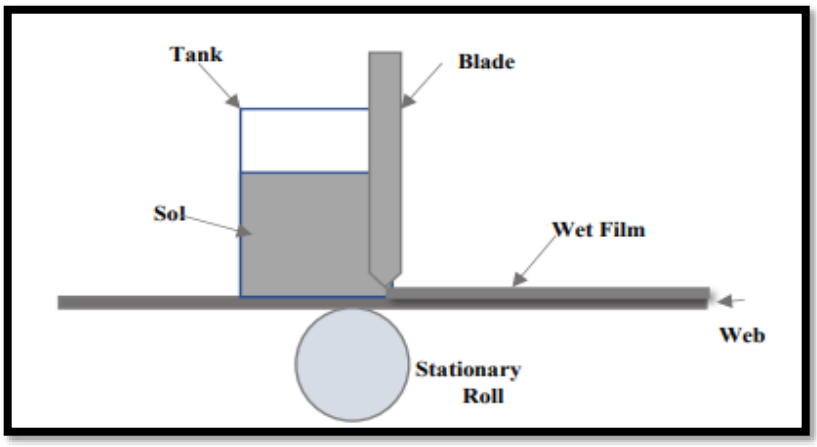

Figure 22.3 Moving Web setup for coating plastic foils[4]

ii) Spiral Film Doctor Blading

Uneven surface coatings and industrial level processes such as foils coatings, textiles and leather coatings are done by Spiral Film Doctor blading. It is used when the moldable material was desired. Spiral applicator is usually used in this technique. Spiral is placed above the substrate. The material is pressed down by the spiral as it rolls over the surface of substrate. The material is also smoothed by the spiral. A S Spiral Film Doctor blading is presented in Figure 3.4.

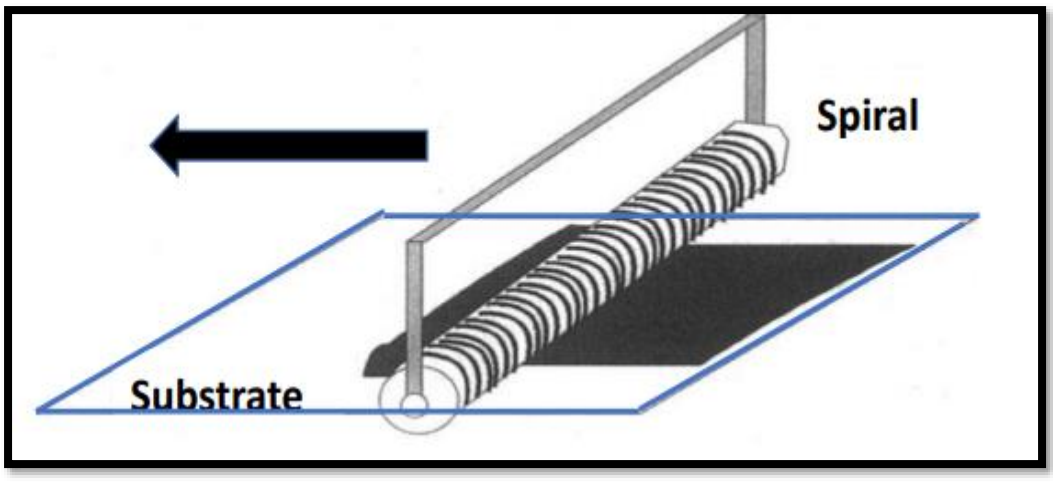

Figure 3.23 Spiral film doctor blade set up[1]

The film thickness is controlled by the gap between the blade and substrates and the geometry of the structure.

3.2.2 Sensitization of Photoanode

3.2.2.1 Traditional Sensitization Method

In this Method, the prepared photoanode is dipped in the dye solution. The metal oxide surface is sensitized using one dye. This affords a much higher level of dye loading. Control parameters in this technique is sensitization time[5].

3.2.2.2 Inject Printed dye sensitization:

For the accurate and control amount of dye on the surface of metal oxide thin films, the inject printing method of concentrated dyes are used. This produces uniform cells with stable and equal performances as compared to drop casting process. Among several advantages of this technique, one is that the controlled amount of dye is injected into the thin film of metal oxide[6].

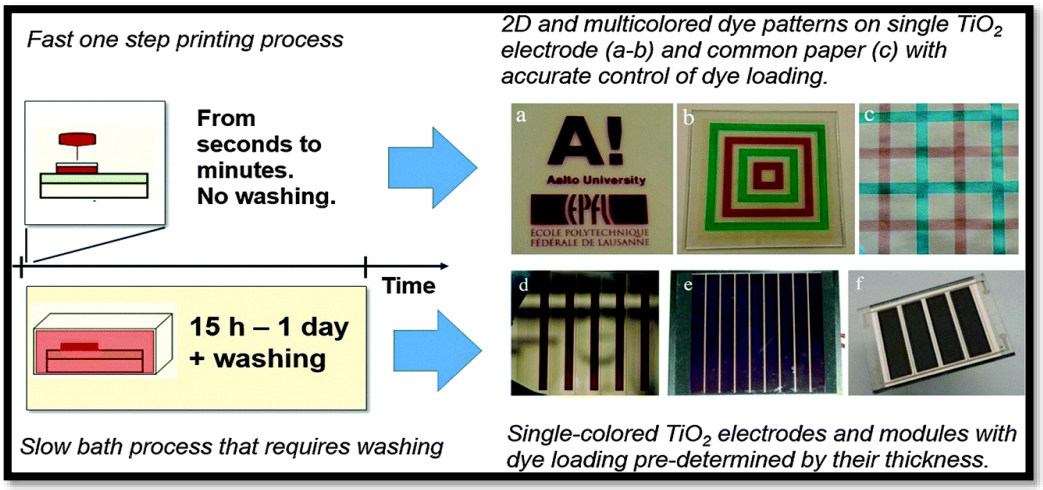

Figure 3.24 Process of Inject printing for DSSC photoanode[7]

3.2.2.3 Functionalized Carboxylate Deposition (FCD)

It is a technique which uses vapor phase deposition of sensitizers. This technique is presented as the alternative of dip coating sensitization method. It is better than dip coating because it forms a monolayer of dye on the metal oxide surface by reducing the dye loading time of the photoanode. The first layer deposition is the spontaneous attachment of the dye molecules with the metal oxide surface. The hydroxyl group are the usual

anchoring ligands of dyes on the surface of metal oxide. The dye molecules are evaporated and attached to the surface of metal oxide chemically by using a covalent bond. As the area of the metal oxide is covered by the deposition of the dye molecules, the process of deposition stops, making it as self-limiting process. The reaction of dye molecule attachment on the surface of titanium dioxide is shown by following reaction:

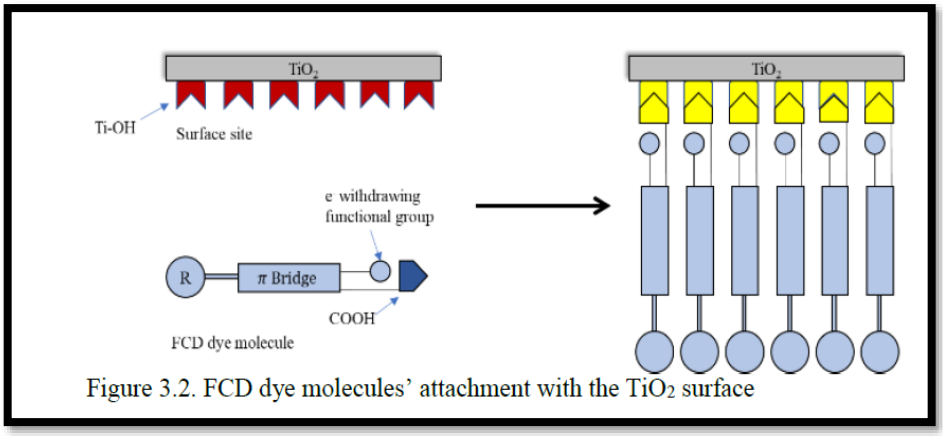

Figure 3.2. FCD dye molecules' attachment with the TiO_2 surface

Figure 3.25 FCD for sensitization of Photoanode in DSSC[8]

$$Ti\text{-}OH + R\text{-}COOH \rightarrow Ti\text{-}COOR + H_2O$$

The advantages of FCD techniques as compared to dip coating are as follow:

1) It decreases up to 95% of dye loading time
2) Solvent use is avoided in this technique
3) Minimum amount of dye is used[9]

3.3 Cell Fabrication

First, all of components are to be made ready as discussed in previous sections. For microfluidic technique, list of all components is given below:

- ✓ Photoanode
- ✓ Counter Electrode
- ✓ Dye
- ✓ Electrolyte
- ✓ Spacer
- ✓ Copper foil
- ✓ Electrolyte injector

For photoanode, a metal oxide, mostly TiO_2/ZnO, are deposited on conductive glass substrates which are FTO/ITO. A standard dye is prepared. Dyes have been discussedin first chapter in details. Dye solution is dissolved in ethanol and sonicated to dispersedye in ethanol. A standard electrolyte, mostly Iodoly AN-150 is used. Platinum coating on FTO glass is used as counter electrode. Two holes are drilled in the counterelectrode. PDMS membrane as spacer is used. For assembling by microfluidic sealing technique [10] following steps are followed and illustration is shown in Figure 3.7.

- ✓ Photoanode is dipped in dye solution and is dipped for 3 hours so that dye is adsorbed in the photoanode
- ✓ The photoanode and counter electrode are placed at some distance by placing spacer in between. The two electrodes are connected by using foils to connect theterminals of both electrodes
- ✓ Electrolyte is filled into the space by injecting through the holes in counter electrode.

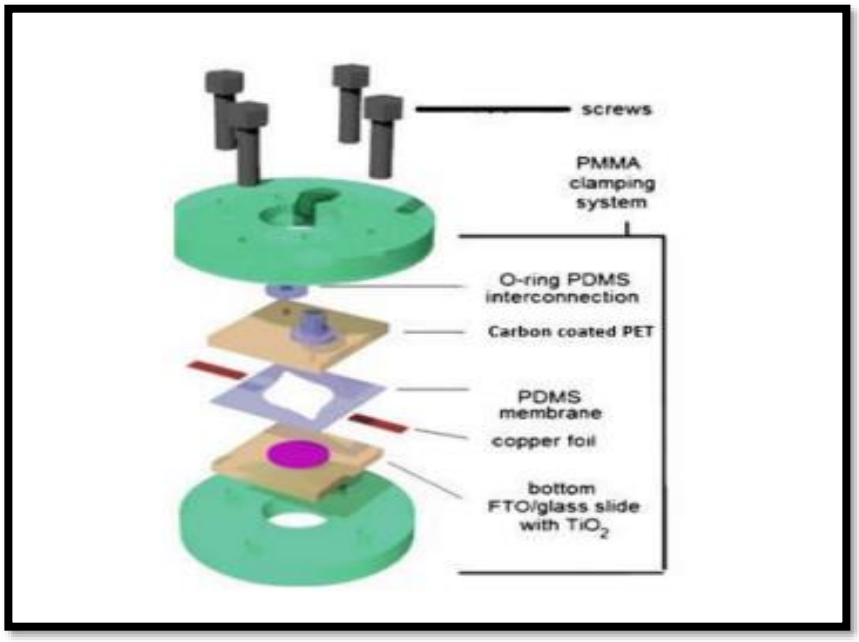

Figure 3.8 Cell Assembly [10]

In this way, DSSC is assembled and then subjected to characterization which will be discussed in later section of characterization techniques.

3.4 Characterization Techniques

There are different characterization techniques to study characteristics of Photoanode, dyes and complete DSSC. UV-vis spectroscopy is used for characterization of dyes, sensitized and co-sensitized photoanode deposited on FTO. Photoanode is also characterized by Profilometry, XRD and Scanning Electron Microscopy. Efficiency of DSSC is measured by solar simulator

3.4.1. UV-vis Spectroscopy

Ultraviolet visible spectroscopy (UV-Vis) is a very popular characterization technique because of its ability to detect almost every molecule. Light in the ultraviolet to visible region illuminates the sample and the amount of light passed through is recorded. This gives us the transmittance behavior of the material and by a simple calculation, the absorbance can also be analyzed. The amount of light absorbed or transmitted at a given wavelength gives us information about the chemical structure of the material under investigation [11].

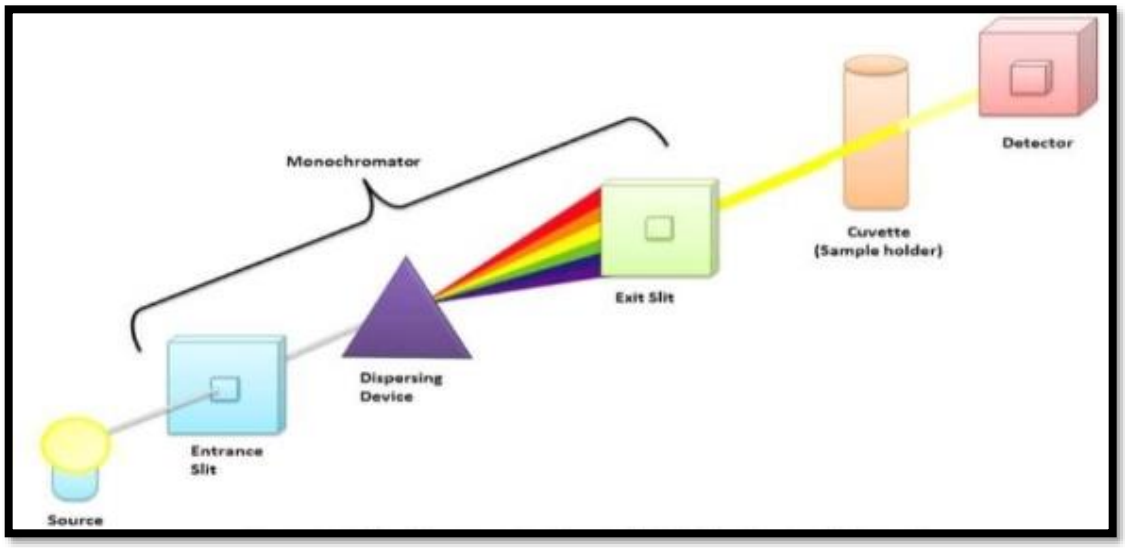

Figure 3.9 Instrumentation of a UV-Vis Spectrophotometer[11]

The technique is often used for general analysis because most elements and compounds can absorb light in that range. The wavelength range for the light used extends from 100 nm (deep UV) to 1000 nm (beyond visible). For this long range of light, typically two different sources are used. The deuterium lamp is for the UV light whereas a tungsten filament produces visible light.

Working Principle

A photon strikes the molecule and after being absorbed excites the molecule to a higher energy state. The UV-Visible light has high energy with the ability to transfer electrons from the highest occupied orbital to an excited state in the lowest unoccupied orbital. The different in energy between both states is the bandgap of the material. The bandgap is unique for each material therefore every crystal structure has its own characteristic absorption spectra.

3.4.2. Diffuse Reflectance Spectroscopy

Diffuse reflectance spectroscopy is a very useful tool for the study of interactions among various formulation components, and the technique has been successfully used in the characterization of many solid-state reactions. [12]. Reflectance spectroscopy is very closely related to UV/Vis spectroscopy, in that both of these techniques use visible light to excite valence electrons to empty orbitals. The difference in these techniques is that in UV/Vis spectroscopy one measures the relative change of transmittance of light as it passes through a solution, whereas in diffuse reflectance, one measures the relative change in the amount of reflected light off of a surface[13].

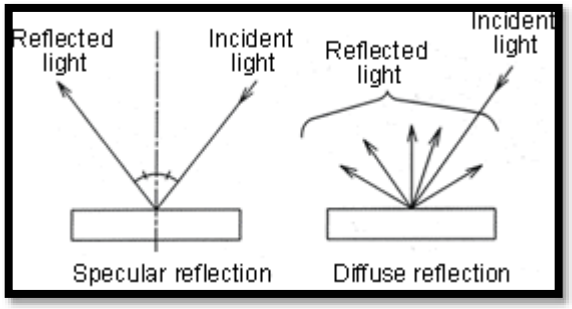

Figure 3.10 Diffuse Reflectance Spectroscopy[14]

Working Principle

As the light strikes the powder sample, it reflects back in all the direction as presented in Figure. 3.11. The reflection that occurs at the surface of powder sample is specular reflection. The powder sample has various shapes present which reflects the light in many the directions. Some of the enters into the powder sample surface and refracted. Scattering of light happen when it enters the surface of powder because of internal refraction. This internal reflection is caused by the powder grain surfaces and recurrent refraction entering

into the powder. The air receives the scattered light as emission. The reflected light becomes less intense as it reflects back or pass though the powder grains and when powder absorbs it. This makes reflected spectrum of diffused light same as the transmission spectrum. But some of the powdered sample absorbs maximum light in which longer wavelength light is absorbs and only shorter wavelength light is reflected back into the air. However, some of the powdered sample did not absorb maximum light and not even long wavelength light is absorbed by this region. Diffuse reflectance from this region has shown high intensity peaks which are significant than transmission spectrum. Nonetheless, the peak intensity of transmission spectrum and diffuse spectrum are contrary as the low intensity peaks of transmission becomes high intensity peaks in diffuse reflectance spectrum. To measure the transmission spectrum or quantitative analysis Kubelka-Munk function id used which is K-M function ($f(R_\infty)$)[14].

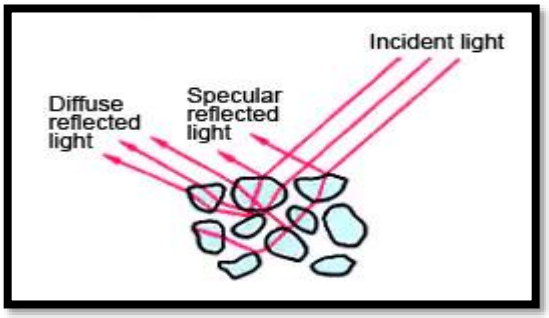

Figure 3.11 Light Scattering from a sample[14]

3.4.3 I-V Characteristic Measurement

The I-V curve is a graph of all possible available combinations of voltage and current operated under constant conditions and give the characteristic electrical properties of a solar cell depending upon the active electrode region that enhances charge transport, exciton dissociation and carrier injection. These properties a usually measured using a Keithley source meter under illuminated and dark conditions. Generally, the I-V curve has a characteristic shape point, the behavior is similar however, when it is to the right of the MPP, there is an immediate decline in power output because of sealed charges within the solar cell that do not flow out. These charges are a result of increased voltage output [15]. IV-curve gives the Isc, Voc and Fill Factor FF for the device under consideration and this information can be used to find efficiency of the cell.

Newport Oriel IV station with Kiethley PVIV 2400 source meter and solar simulator under power intensity of 750 W/m2 were used for IV measurements. While the cell was covered with a black mask having an active area of 0.22 cm2 to limit extra light [16]. The simulator's output light intensity was calibrated (1000 Wm-2) using a reference Si photodiode that Newport 36 had calibrated at (1000 W m-2). Important characteristics such as open circuit voltage (Voc), short circuit current density (Jsc), fill factor (FF), and photo conversion efficiency can be calculated using the J-V data measured for samples.

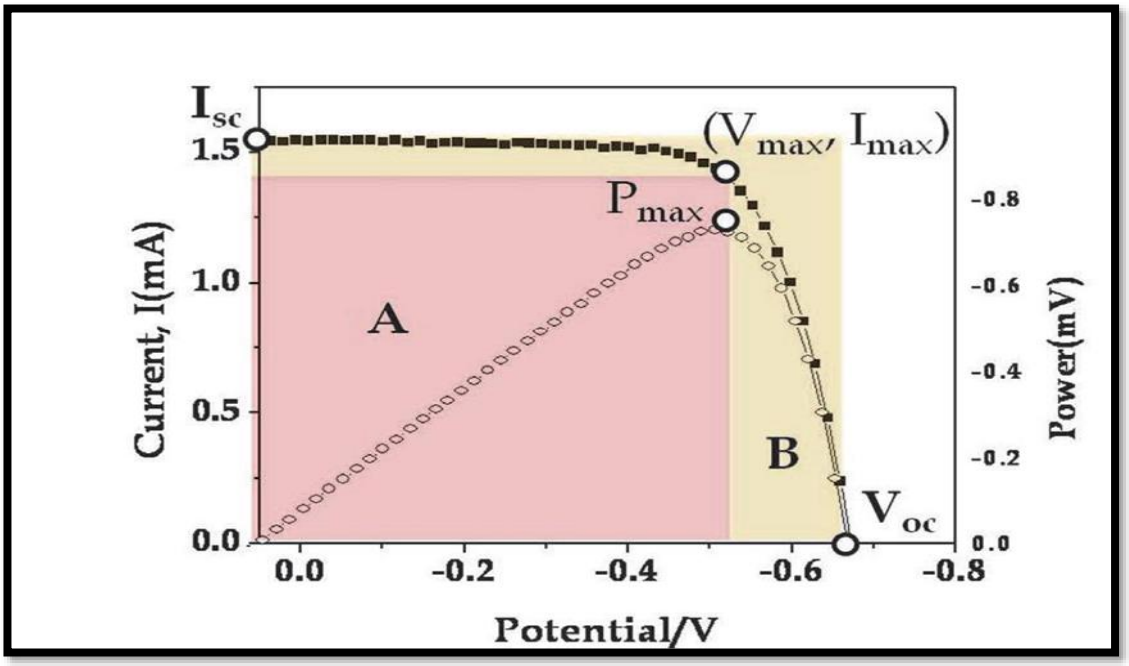

Figure 3.12 I-V Curve and different parameters of DSSCs with output Current and Power as a function of Voltage[17]

CHAPTER SUMMARY

All the experimental techniques and characterization techniques used in this research work have been discussed in detail in this chapter. Fabrication techniques of electrodes for DSSCs assembly and for characterization have been discussed. Doctor blade technique for electrode fabrication has been explained. Different characterization techniques, UV/Vis spectroscopy, diffuse reflectance spectroscopy and Solar Simulator for IV Characteristic curve for DSSC characterization have been described.

References

[1] A. Berni, M. Mennig, and H. Schmidt, “2.2.8 DOCTOR BLADE.”

[2] P. H. Gaskell, B. Rand, J. L. Summers, and H. M. Thompson, “The effect of reservoir geometry on the flow within ceramic tape casters,” *J. Eur. Ceram. Soc.*, vol. 17, no. 10, pp. 1185–1192, Jan. 1997.

[3] R. RUNK and A. MJ, “A PRECISION TAPE CASTING MACHINE FOR FABRICATING THIN CERAMIC TAPES,” *A Precis. TAPE Cast. Mach. Fabr. THIN Ceram. TAPES*, 1975.

[4] A. Berni, M. Mennig, and H. Schmidt, “Doctor Blade,” *Gravure*, vol. 21, no. 1, pp. 89–92, Feb. 2004.

[5] J. M. Cole, G. Pepe, O. K. Al Bahri, and C. B. Cooper, “Cosensitization in Dye-Sensitized Solar Cells,” *Chem. Rev.*, vol. 119, no. 12, pp. 7279–7327, Jun. 2019.

[6] S. G. Hashmi *et al.*, “Dye-sensitized solar cells with inkjet-printed dyes,” *Energy Environ. Sci.*, vol. 9, no. 7, pp. 2453–2462, Jul. 2016.

[7] S. G. Hashmi *et al.*, “Dye-sensitized solar cells with inkjet-printed dyes,” *Energy Environ. Sci.*, vol. 9, no. 7, pp. 2453–2462, Jul. 2016.

[8] M. A. Mamun, “A Route to Fabricate Rapid and Efficient Dye-sensitized Solar Cells through Minimizing the Duration of TiO2 Film Disposition and Dye Sensitization,” *Electron. Theses Diss.*, Jan. 2018.

[9] A. Mamun, “A Route to Fabricate Rapid and Efficient Dye-sensitized Solar Cells A Route to Fabricate Rapid and Efficient Dye-sensitized Solar Cells through Minimizing the Duration of TiO2 Film Disposition and Dye through Minimizing the Duration of TiO2 Film Disposition and Dye Sensitization Sensitization.”

[10] S. Sa, “Platisol T / SP Platisol T / SP,” no. 1, pp. 2–7, 2011.

[11] “Ultraviolet-Visible (UV-Vis) Spectroscopy | Protocol.” .

[12] H. G. Brittain, “Solid-State Analysis,” *Sep. Sci. Technol.*, vol. 3, no. C, pp. 57–84, Jan. 2001.

[13] “solid state chemistry - What is the principle of diffuse reflectance spectroscopy behind band gap measurement? - Chemistry Stack Exchange.” [Online]. Available: https://chemistry.stackexchange.com/questions/6091/what-is-the-principle-of-diffuse-reflectance-spectroscopy-behind-band-gap-measur. [Accessed: 19-May-

2022].

[14] “ABC’s of the Diffuse Reflection Method : SHIMADZU (Shimadzu Corporation).” [Online]. Available: https://www.shimadzu.com/an/service-support/technical-support/analysis-basics/ftirtalk/talk1.html. [Accessed: 19-May-2022].

[15] and Kohichi Maeda, Jin-ichi Ikemoto, Fumiro Tsuruda and Teruo Takeda, “Intelligent Instrument Streamlines dc Semiconductor Parameter Measurements.”

[16] C. Zhao *et al.*, “Low temperature growth of hybrid ZnO/TiO2 nano-sculptured foxtail-structures for dye-sensitized solar cells,” *RSC Adv.*, vol. 4, no. 105, pp. 61153–61159, Nov. 2014.

[17] J.-J. Lee, M. M. Rahman, S. Sarker, N. C. D. Nath, A. J. S. Ahammad, and J. K. Lee, “Metal Oxides and Their Composites for the Photoelectrode of Dye Sensitized Solar Cells,” *Adv. Compos. Mater. Med. Nanotechnol.*, Apr. 2011.

Chapter 4

Experimentation

4.1 Introduction

In this Chapter, Experimentation techniques are discussed in detail. The steps for preparation of photoanode, sensitization of photoanode and fabrication of dye sensitized solar cells are discussed with steps to prepare photoanode, counter electrode, dye solution and sensitization of dyes.

4.2 Materials

4.2.1 Materials used for ZnO nanorice Synthesis

Materials used for the synthesis of ZnO nanorice are Zinc Acetate dihydrate (Sigma Aldrich), Sodium Hydroxide pellets (Sigma Aldrich), Methanol (Merck), and Deionized water. These chemicals are used without further purification.

4.2.2 Solvents used for Dye solution preparation

Solvents used for dye solution preparation are dimethyl formamide (DMF) (Sigma Aldrich), Acetonitrile (Duksan Pure Chemicals). These chemicals were used without further purification.

4.2.3 Solvents used for washing of FTOs

Solvents used for the washing of fluorine-doped tin oxide glass substrate (FTO) are Distilled Water, Sulfuric acid (Sigma Aldrich), Hydrogen peroxide (BDH), Ethanol (BDH), isopropanol (BDH) and Acetone (BDH). These solvents were used without further purification.

4.2.4 Materials used for photoanode preparation

Materials used for the fabrication of semiconductor metal oxide photoanodes are synthesized ZnO nanorice, dimethyl formamide (DMF) (Sigma Aldrich), fluorine-doped tin oxide glass substrate [F: SnO_2, 8 Ω/cm^2] (Sigma Aldrich) and Nafion. The FTOs are cleaned before the deposition of ZnO nanorice film. Both these solvents are used for preparation of the slurry of ZnO nanorice.

4.2.5 Materials used for Counter Electrode preparation

Fluorine-doped tin oxide glass substrate [F: SnO_2, 8 Ω/cm^2] (Sigma Aldrich), and Platinum paste (Platisol T/SP) (solaronix) are used in the fabrication of counter electrode by doctor blading platinum paste on the FTO followed by annealing.

4.2.6 Materials used for DSSC fabrication

Electrolyte Iodolyte AN50 (Solaronix), prepared photoanode, Prepared counter electrode and copper strips (locally purchased) are used for the fabrication of DSSC fabrication.

4.3 Synthesis of Zinc Oxide (ZnO) nanoparticles

Zinc oxide was prepared by reported hydrothermal method [1]. 1M solution of zinc acetate in Methanol. 3M NaOH solution was prepared in menthol separately by stirring. The anionic solution was added drop wise in zinc acetate solution while stirring and maintaining the pH between 9 to 11. This solution was autoclave for 12 hours and after that solution was rinse and washed by ethanol and distilled water several times. The resulted slurry was dried overnight in the oven. The dried powder was grinding in mortal and pastel for 30mins.

4.4 Fabrication of Photoanode

4.4.1 Cleaning of FTO

Transparent conducting oxide (TCO) glass was used as the base of photoanode. Fluoride doped tin oxide (FTO) conducting glass as a substrate, which was cleaned in water, isopropanol, acetone and ethanol under sonication for 15 minutes respectively[2][3]. Prior to this, the FTO substrate are washed with soap and piranha solution prepared by sulfuric acid and hydrogen peroxide to remove organic residue from the substrate in ultrasonic bath[4][5]. Followed by cleaning with distilled water and isopropanol[6] in the same order to avoid the formation of ester on the surface of substrates. The cleaned glass was then kept in isopropanol for 24 hours prior to use for film deposition.

4.4.2 Preparation of ZnO Paste

ZnO paste was prepared using25mg of synthesized ZnO nanorice mixed with 0.5ml of dimethyl formamide (DMF) [7] containing25 μL of 5 wt% Nafion as a binder to help in adhesion [8] under sonication to make a slurry.

4.4.3 Deposition of Photoanode

Clean FTO with conductive side upward were placed on a clean surface. A locally purchased non residual adhesive tape with a circle of area 0.78cm^2 was placed on the conductive surface of FTO[9]. The slurry was then dip-coated onto cleaned FTO glass substrate and tape casting technique employed to ensure the same thickness[10]. The drop casted photoanodes were left overnight for air drying. After air drying, the electrode was annealed at 350°C[11] for 30 minutes [12].

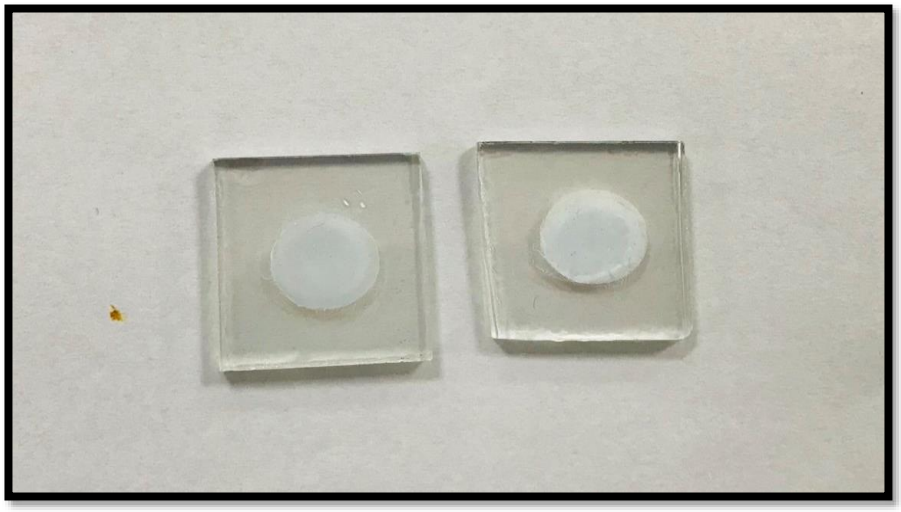

Figure 4.26 Prepared Photoanode with ZnO nanorice

4.5 Fabrication of Counter Electrode

Counter electrode was prepared on FTO with hole punched for introduction of electrolyte. The holes were drilled through with the help of diamond drilling bit. Platisol D/SP(Solaronix) solution by doctor blade technique [13] was deposited on FTO with holes[14] followed by annealing for 30 mins.

4.6 Preparation of Dye Solution

Dye solutions of different dyes are prepared in different solvents. The details of solvents along with concentrations are presented in the following table. These solutions are sonicated up to 45 mins in ultraviolet sonicator.

Table 4.1 Dye solution Data

Dye Name	Solvent	Concentration (mM)
SZD-1	DMF	0.2
SZD-2	DMF	0.2
SZD-3	DMF	0.2
SZD-4	DMF	0.2
SMA-06	Acetonitrile	0.2
PT4N	Acetonitrile	0.2

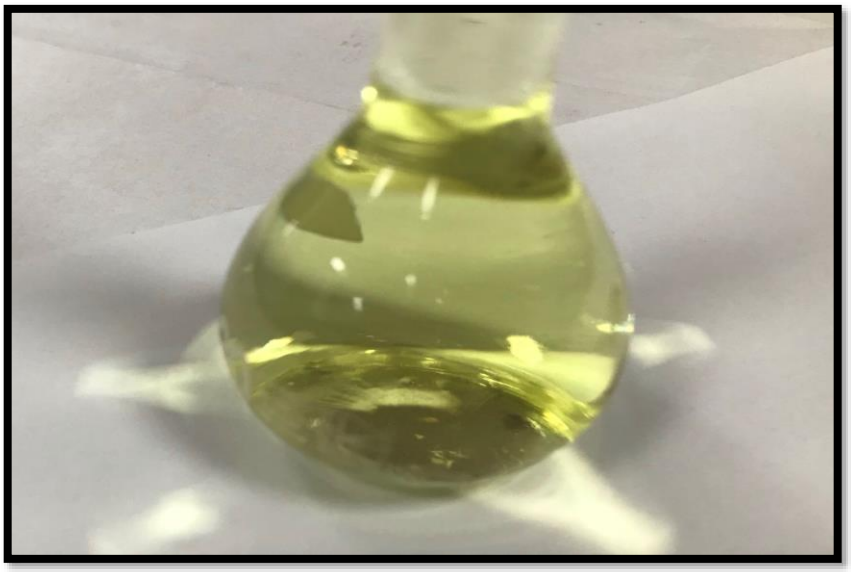

Figure 4.27 Prepared solution of PT4N

4.7 Characterization of Dyes

All of the dyes were characterized by UV-Vis NIR Spectrophotometer (UV-3600 Plus) to find the absorbance of the dye solutions.

4.8 Sensitization of Photoanode

The photoanodes are sensitized in dyes for 3 hours at room temperature used in dye sensitized solar cells as depicted in Figure.4.1. Samples then were rinsed with respective solvents to wash out un-adsorbeddye [22].

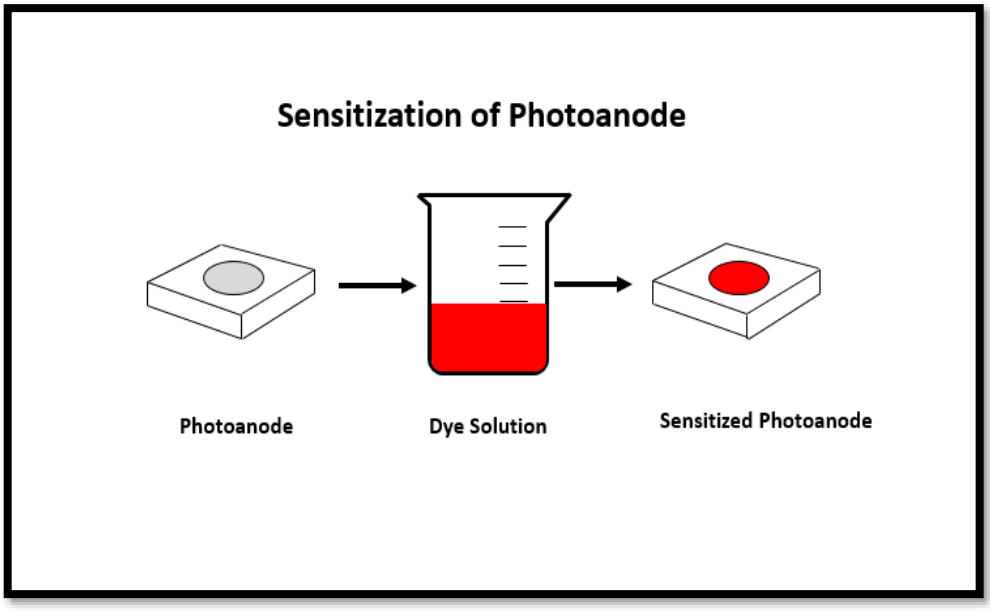

Figure 4.28 Photoanode Sensitization

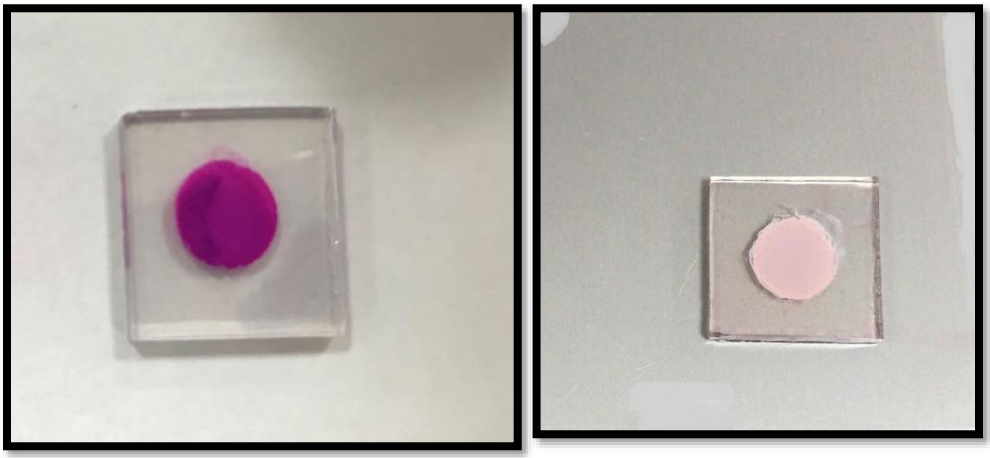

Figure 4.29 Photoanode Sensitized by SMA-06 and SZD-1

4.9 Characterization of Sensitized Photoanode

These sensitized photoanodes were characterized by characterized by UV-Vis NIR Spectrophotometer (UV-3600 Plus) to find the absorbance of dye adsorbed photoanode.

4.10 Assembling Dye Sensitized Solar Cell

DSSCs were assembled using microfluidic structure [23] with I^-/I^{3-} redox couple electrolyte. ZnO based photoanode and Platinum coated counter electrodes were used. The two electrodes were clipped together with a spacer (PMMA/PDMS) used in between the two electrodes. The spacer function is to avoid short circuiting and separate the two

electrodes. Copper strips were used to makeconnections for both photoanode and counter electrode[24]. Electrolyte was injected into the assembly by using an injection[25]. The electrolyte was injected through holes drilled in counter electrodes. All the assembled DSSCs having an active area of 0.78cm^2 and electrical measurements were performed by applying a black mask with an active area 0.22cm^2.

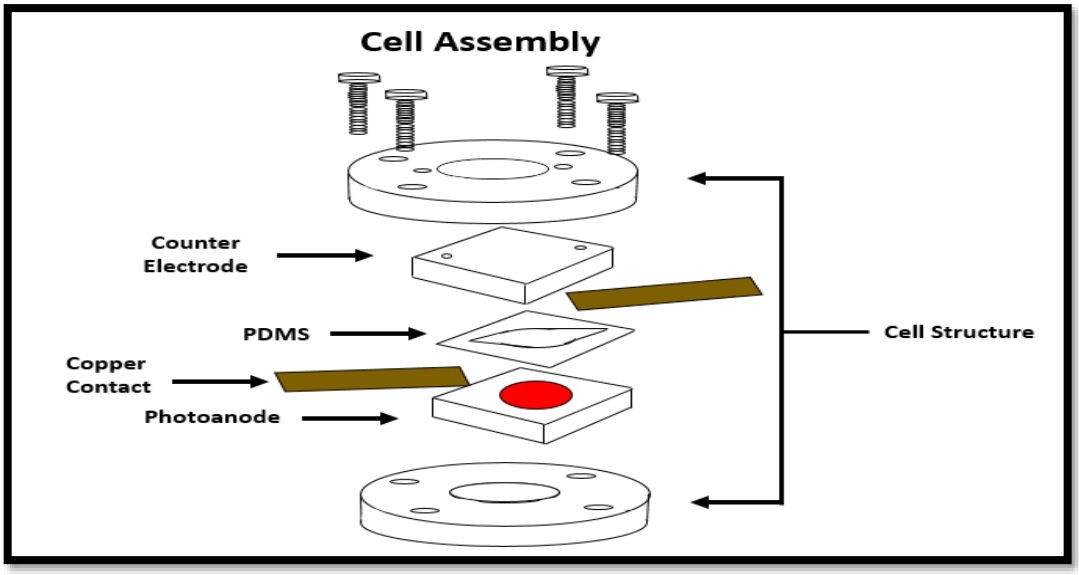

Figure 4.30 Cell Assembly for DSSC

4.11 Characterization of DSSCs

Characterization of Fabricated devices were done by Newport Oriel IV station with Keithley PVIV 2400 solar simulator for IV cure measurements.

Figure 4.31 Fabricated DSSC by using microfluidic structure

Chapter Summary

This Chapter Discussed the methodology, techniques and equipment used in the fabrication of dye sensitized solar cells. Different dyes are prepared in different solvents which are defined along with concentrations for best performance in DSSC. The preparation of photoanode, sensitization and counter electrode along with assembling DSSCs with microfluidic structure are explained.

References

[1] A. H. Javed *et al.*, "Effect of ZnO nanostructures on the performance of dye sensitized solar cells," *Sol. Energy*, vol. 230, pp. 492–500, Dec. 2021.

[2] V. More, V. Shivade, and P. Bhargava, "Effect of Cleaning Process of Substrate on the Efficiency of the DSSC," vol. 75, no. 1, pp. 59–62, Jan. 2016.

[3] "(PDF) FABRICATION OF GRAPHENE OXIDE/ZINC OXIDE NANOCOMPOSITE THROUGH SPRAYING METHOD FOR SOLAR CELL APPLICATION." [Online]. Available: https://www.researchgate.net/publication/341204030_FABRICATION_OF_GRAPHENE_OXIDEZINC_OXIDE_NANOCOMPOSITE_THROUGH_SPRAYING_METHOD_FOR_SOLAR_CELL_APPLICATION. [Accessed: 09-Jun-2022].

[4] P. Stevic, "Piranha Cleaning Standard Operating Procedure," 2018.

[5] N. Shahzad, Z. Shah, M. I. Shahzad, K. Ahmad, and D. Pugliese, "Effect of seed layer on the performance of ZnO nanorods-based photoanodes for dye-sensitized solar cells," *Mater. Res. Express*, vol. 6, no. 10, Aug. 2019.

[6] K. Gossen and A. Ehrmann, "Influence of FTO glass cleaning on DSSC performance," *Optik (Stuttg).*, vol. 183, pp. 253–256, Apr. 2019.

[7] K. Davis, R. Yarbrough, M. Froeschle, J. White, and H. Rathnayake, "Band gap engineered zinc oxide nanostructures via a sol–gel synthesis of solvent driven shape-controlled crystal growth," *RSC Adv.*, vol. 9, no. 26, pp. 14638–14648, May 2019.

[8] F. Lufrano, P. Staiti, and M. Minutoli, "Influence of Nafion Content in Electrodes on Performance of Carbon Supercapacitors," *J. Electrochem. Soc.*, vol. 151, no. 1, p. A64, Dec. 2004.

[9] S.-Y. Kwon, W. Yang, and Z. Zhou, "DSSCs Efficiency by Tape Casting Pt Counter Electrode and Different Thickness Between Two Substrates," *J. Korean Inst. Electr. Electron. Mater. Eng.*, vol. 26, no. 3, pp. 209–215, Mar. 2013.

[10] M. E. Mofdal, N. M. Osman, N. O. Khalifa, N. A. Eassa, N. H. Talib, and H. A. Albushra, "The Effect of the Substrate Type on ZnO Nanoparticles Dye Sensitized

Solar Cell," *2018 Int. Conf. Comput. Control. Electr. Electron. Eng. ICCCEEE 2018*, Oct. 2018.

[11] A. Al-Kahlout, "Thermal treatment optimization of ZnO nanoparticles-photoelectrodes for high photovoltaic performance of dye-sensitized solar cells," *J. Assoc. Arab Univ. Basic Appl. Sci.*, vol. 17, pp. 66–72, Apr. 2015.

[12] P. P. Das, S. Mukhopadhyay, S. A. Agarkar, A. Jana, and P. S. Devi, "Photochemical performance of ZnO nanostructures in dye sensitized solar cells," *Solid State Sci.*, vol. 48, pp. 237–243, Oct. 2015.

[13] S. Sa, "Platisol T / SP Platisol T / SP," no. 1, pp. 2–7, 2011.

[14] P. Widiatmoko, H. Devianto, I. Nurdin, A. Adriaan, and H. N. Purwito, "THE EFFECT OF COUNTER ELECTRODE PREPARATION METHODS TOWARD DYE SENSITIZED SOLAR CELL PERFORMANCE," *J. Teknol. Bahan dan Barang Tek.*, vol. 8, no. 1, p. 1, Jun. 2018.

[15] Z. Wan, C. Jia, Y. Wang, and X. Yao, "A Strategy to Boost the Efficiency of Rhodanine Electron Acceptor for Organic Dye: From Nonconjugation to Conjugation," *ACS Appl. Mater. Interfaces*, vol. 9, no. 30, pp. 25225–25231, Aug. 2017.

[16] X. Qian, L. Lu, Y. Z. Zhu, H. H. Gao, and J. Y. Zheng, "Triazatruxene-based organic dyes containing a rhodanine-3-acetic acid acceptor for dye-sensitized solar cells," *Dye. Pigment.*, vol. 113, pp. 737–742, Feb. 2015.

[17] J. Pei *et al.*, "Triphenylamine-based organic dye containing the diphenylvinyl and rhodanine-3-acetic acid moieties for efficient dye-sensitized solar cells," *J. Power Sources*, vol. 187, no. 2, pp. 620–626, Feb. 2009.

[18] T. Y. Wu *et al.*, "Iranian Chemical Society Synthesis and Characterization of Three Organic Dyes with Various Donors and Rhodanine Ring Acceptor for Use in Dye-Sensitized Solar Cells," *J.*, vol. 7, no. 3, pp. 707–720, 2010.

[19] T. Marinado *et al.*, "Rhodanine dyes for dye -sensitized solar cells : spectroscopy , energy levels and photovoltaic performance," *Phys. Chem. Chem. Phys.*, vol. 11, no. 1, pp. 133–141, Dec. 2008.

[20] C. A. Echeverry *et al.*, "Organic dyes containing 2-(1,1-dicyanomethylene)rhodanine as an efficient electron acceptor and anchoring unit for dye-sensitized solar cells," *Dye. Pigment.*, vol. 107, pp. 9–14, Aug. 2014.

[21] C. A. Echeverry, M. Á. Herranz, A. Ortiz, B. Insuasty, and N. Martín, "Rhodanine-3-acetic acid and π-extended tetrathiafulvalene (exTTF) based systems for dye-sensitized solar cells," *New J. Chem.*, vol. 38, no. 12, pp. 5801–5807, Nov. 2014.

[22] J. Fang, H. Fan, H. Tian, and G. Dong, "Morphology control of ZnO nanostructures for high efficient dye-sensitized solar cells," *Mater. Charact.*, vol. 108, pp. 51–57, Oct. 2015.

[23] N. Shahzad *et al.*, "Monitoring the dye impregnation time of nanostructured photoanodes for dye sensitized solar cells," *J. Phys. Conf. Ser.*, vol. 439, no. 1, p. 012012, Jun. 2013.

[24] U. Rau and T. Kirchartz, "Charge Carrier Collection and Contact Selectivity in Solar Cells," *Adv. Mater. Interfaces*, vol. 6, no. 20, p. 1900252, Oct. 2019.

[25] J. Wu *et al.*, "Electrolytes in dye-sensitized solar cells," *Chem. Rev.*, vol. 115, no. 5, pp. 2136–2173, Mar. 2015.

Chapter 5

Results and Discussions

5.1 Introduction

This chapter presents the results obtained by characterizations of Ruthenium and Organic dyes used in ZnO-based dye Sensitized solar cells. It describes the performance of these dyes by elaborating the function of species presents in the dye and causes of different behaviors presented by it.

5.2 Morphology of Nanoparticles

The structural analysis of grown nanostructure has been performed by X-ray diffractometer and obtained results are presented in Figure 2 which have confirmed the growth of the ZnO wurtzite phase. The peak obtained at 2θ equate to 31.5°, 34.2°, 36.0°, 47.2°, 56.4°, 62.7°, 66.2°, 67.7° and 68.9° indicate the reflection from the planes (001), (002), (101), (102), (110), (103), (200), (112) and (201) respectively which coincide with the reported standard data (PDF # 99-0111) and a previously conducted study [1]. Further, the sharp peaks obtained during XRD analysis are an indication of a more crystalline

structure. No additional peak except peaks for ZnO wurtzite phase was observed during the analysis which reveals that no impurity is present in the final product.

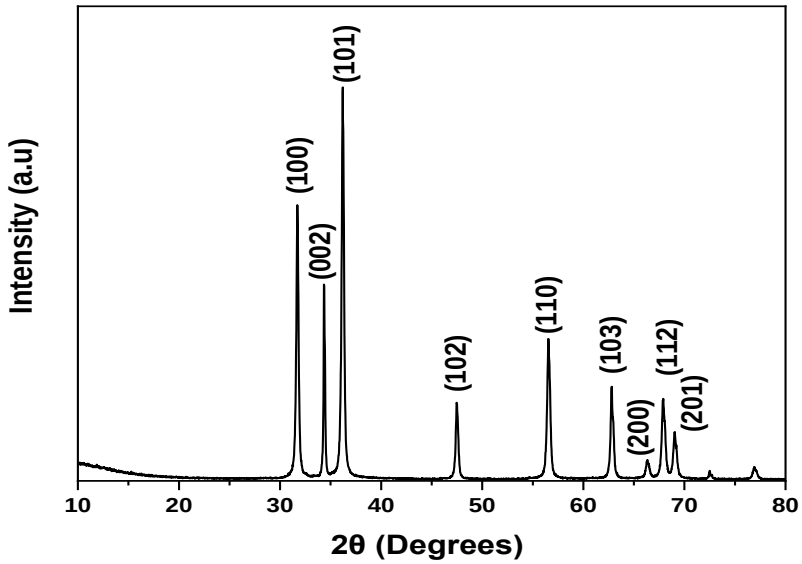

Figure 5.32 XRD Pattern of grown ZnO nanorice

Morphological changes were assessed with the help of scanning electron microscopy and depicted in Figure 3(a). The images uncovered that the ZnO nanostructures possess a nanorice-like morphology and are stacked on each other in irregular manners. All the grown nanostructures acquired uniformity in size ranging from 112-200 nm with an average particle size of 145 nm. The small particle size of nanostructures is a sign of more surface area which helped the dye adsorption onto photoanodes. Moreover, the 1D growth of nanostructures has shown better conductivity as observed in our previous study [2]. Corresponding elemental analysis of grown photoanodes is illustrated in Figure 3(b) and

shows the presence of Zinc (Zn) and Oxygen (O) in the ZnO matrix while the presence of Ca and Si is associated with the glass substrate on which ZnO film was deposited.

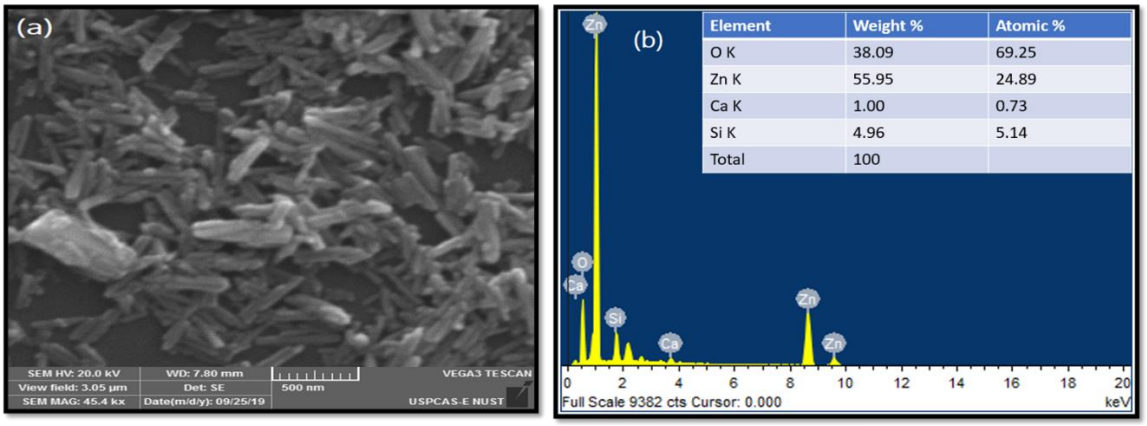

Figure 5.33 (a) SEM image of ZnO grown nanostructure film on a glass substrate (b) Elemental analysis of ZnO film over a glass substrate

5.3 Optical Properties of Dye Solutions

The absorbance of dyes was measured by UV-Vis NIR Spectrophotometer (UV-3600 Plus) which is illustrated in Figure 4(a). Ruthenium-based dyes have shown absorption ranging from 350nm up to 700nm. Among ruthenium-based dyes, SZD-3 has shown the highest absorption. It has a peak at 407 nm along with an elbow at 372 nm. The lowest absorption is shown by SZD-2 which has a minor peak at 320 nm. SZD-1 along with the absorption peak in the visible region at 530 nm has shown a peak in the UV region at 319 nm while SDZ-4 has shown an absorption peak in the UV region at 319 nm. The peaks in high energy wavelength in the range of 300 to 350 nm of all these dyes are attributed to intraligand **π-π*** transition [3] and lower energy peaks in the range of 400nm to 600nm of these dyes are the outcome of metal to ligand charge transfer (MLCT) [4]. Among the organic dyes, PT4N has the absorption peak at 380nm and on contrary, SMA-06 has the absorption peak at 526 nm. Peaks of these dyes in the higher energy region are because of the **π-π*** of aromatic nuclei present in the dyes and the lower energy visible region is due to intermolecular charge transfer [5]. Photoluminescence emission spectra of all dyes were also recorded with the help of a Photoluminescence spectrophotometer and presented in Figure 4(b). All of the Ruthenium dyes SZD-1, SZD-2, SZD-3, and SZD-4 have shown emissions in the visible and near-infrared regions. The SZD-1, SZD-2, SZD-3, And SZD-4 have excitation peaks at 410, 390, 370, and 410 nm resulting in emission peaks at 826,

796, 865, and 822 nm respectively. All these dyes have carboxylic acid and SCN present in their structure and the red Shift of emission happened because the energy of ligand **π*** is orbital decreases attributing to the Carboxylate electron-withdrawing properties [6]. Sigma donation of NCS^- is also responsible for the red shift due to the stabilization of the Center atom of Ru during the excitation state of MLCT [7][8]. Dicyanoisophorone dye SMA-06 has shown an emission peak of 678 nm at a 460 nm excitation peak. A red shift of organic dye SMA-06 is owing to the presence of carboxylic-linked benzene which decreased the electron donating capacity of the molecule [5]. Rhodaniane Dye PT4N has excitation at 390 nm and an emission peak at 824 nm. The red shift of emission is caused by the presence of phenyl molecule as electron accepting moiety [9]. Further, among the Ruthenium based dyes, SDZ-2 and SDZ-4 have shown the highest emission peaks which can be attributed to the absorption of these dyes in high-energy regions that can generate more electron-hole pairs while among the organic dye SMA-06 has shown the highest emission peak that is possibly due to the extended absorption from UV to visible region.

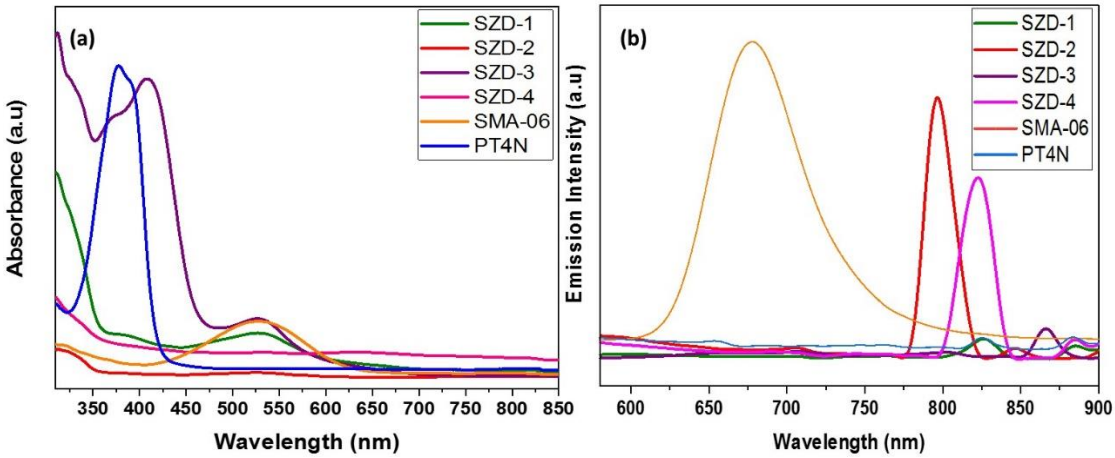

Figure 5.34 (a) Absorption spectra of dyes (a) Photoluminescence emission spectra of dyes

The diffuse reflectance Spectroscopy was used to record the absorption data for pristine photoanodes and dye-adsorbed photoanodes and the obtained results are depicted in Figure 5(a,b). Pure ZnO photoanode has shown an absorption edge in the UV region with a bandgap of 3.31 eV, which is later extended to the visible region after dye adsorption, and no other peak is observed in the visible region for pristine ZnO photoanode [2]. Although the large surface area of the ZnO nanorice-like structure harvests a larger portion of light by increasing the traveling path of light and improving the dye molecule-photoanode interaction in addition to appropriate dye loading.[10]. The peak at 380 nm of

PT4N related to intraligand **π-π*** transition is reduced after anchoring on the metal-oxide surface as compared to SMA-06 which has a red shift in the peak from 526 nm to 540 nm. The ruthenium dye series of SZD-1, SZD-2, SDZ-3, and SDZ-4 has shown similar results of absorbance in sensitized photoanode even the intensity of SDZ-3 is reduced which having the extended absorbance spectra along with more intensity.

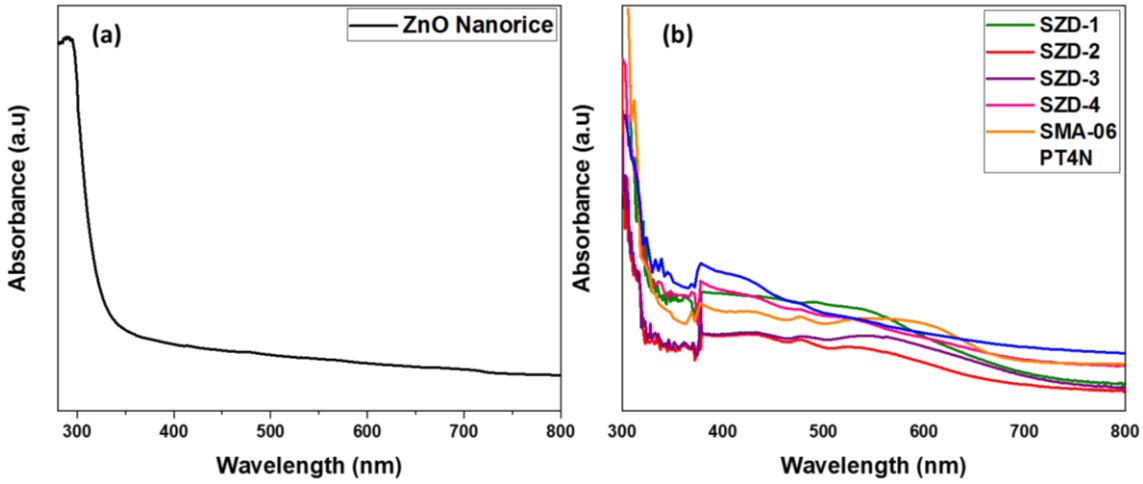

Figure 5.35 (a) Pristine ZnO nanorice-based photoanode (b) Dye adsorbed photoanodes

5.4 Photovoltaic Properties of Solar Cells

The fabricated devices are tested under standard testing conditions and the results are illustrated in Figure 6. Open circuits voltage Voc, Short Circuit current density Jsc, and efficiency of the fabricated devices are summarized in Table.2. The performance of the DSSC is dependent on the ZnO surface, structure, porosity for dye absorption, and shape and size of particles [11]. The highest efficiency is being observed for SZD-3 with an open-circuit voltage of 0.51 volts and a short circuit current density of 4.76 mA/cm^2. In SZD-3, the Nitrogen donor corresponds with Ruthenium metal as well as with the amine nitrogen and azomethine nitrogen [12]. The SZD-3 has multiple anchoring groups having nitro and Carboxyl group. These anchoring groups increased the binding properties of dyes to the ZnO surface [12] which consequently increases the efficiency of the devices. All the ruthenium dyes except SZD-4 have shown higher efficiencies than Organic dyes. Although, SZD-4 has shown the highest absorbance in sensitized photoanode which is possibly owing to two amino group units present in the SZD-4 dye makes it is less efficient than SZD-2 having only one amino group [13]. Amine group anchoring on the ZnO surface is less lasting than the nitro group. Further, The electron recombination is higher,

the short lifetime of electron and higher resistance [13] in SZD-4 in comparison with SZD-3. SZD-4 dye sensitization was also limited like other dyes on the ZnO photoanode and went through the phenomena of bleaching of photoanode which is caused by ZnO and dye molecule weaker molecular bonding. This insufficient dye molecule bonding on the surface of photoanode causes a higher recombination rate, lesser free-electron availability, and conversion of porous structure into denser structure [14]. SZD-1 has shown lower efficiency than SZD-3 likely due to one nitro group presence in the molecule. The ZnO particle may undergo the conversion into Zn^{2+} that can decrease the performance of DSSC and reduces the efficiency of the cell due to the acidic dye adsorption on the ZnO surface that likely makes a layer of Zn^{2+}/dye molecule which act as an insulating layer stopping the electron transfer from the dye to metal oxide surface [15]. Zn^{2+}-Ru dye agglomeration on the surface of the ZnO photoanode is responsible for charge transfer loss from dye to metal oxide resulting into the recombination [14] of charge and reducing the output of the fabricated device.

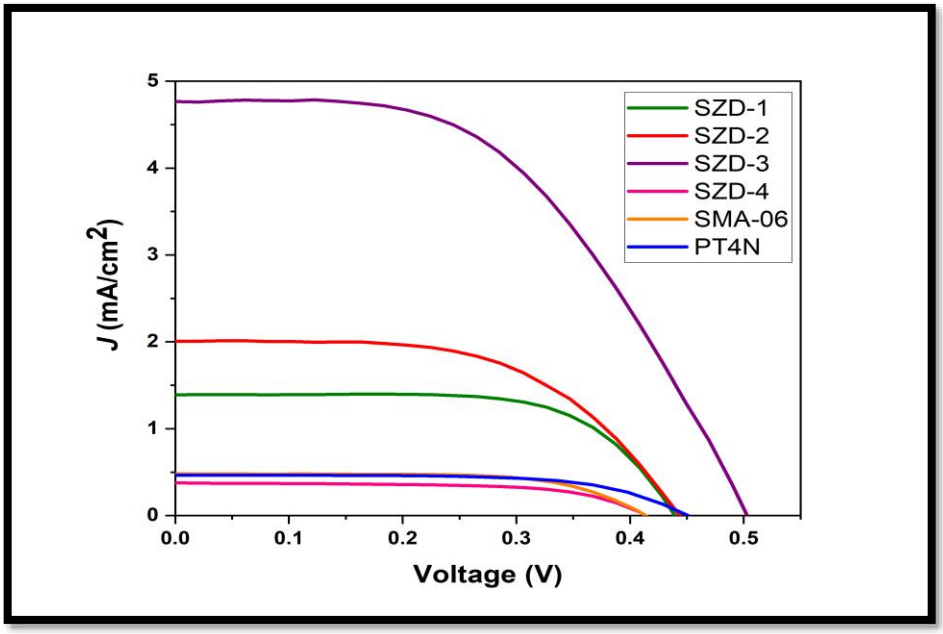

Figure 5.36 Photovoltaic Characteristics of Solar cells by using different dyes

These lower efficiencies are because of the contribution of charge recombination which is induced by grain boundaries and disordered particles [16] as well as water-induced desorption of dye molecule from the ZnO surface [17]. Ru-dye sensitized ZnO photoanodes are less efficient because of the strong basic nature of photoanode and the

strong acidic nature of dye [18]. Both organic dyes have almost the same open-circuit voltages, short circuit current densities, and comparable efficiencies. Rhodanine sensitizers have shown less photovoltaic efficiency due to a single anchoring group present in the molecule, although the sensitized photoanode has more absorbance than ruthenium dyes. This could be because of the dye aggregation on the photoanode surface [19] that hinders the photovoltaic performance of fabricated devices due to electron transfer difficulty [20]. This aggregation of dye molecules reduced the efficiency of dye as well as the performance of DSSC by decreasing the light absorbance on the photoanode as molecules randomly attached to the ZnO surface making a cluster of molecules where the only upper surface of the dye is used to capture the sunlight [21]. The lower output of Jsc and Voc is also because of the surface states and bulk traps in the ZnO surface that increase the recombination of the electron[22]. The electrolyte and metal oxide interface because of unsensitized ZnO surfaces is also a cause of recombination between free electrons of ZnO photoanode and holes in electrolyte[23]. ZnO electron injection kinetics is slower which is also responsible for the high recombination rate[18] in the fabricated device.

Table 5.2 J-V characteristics of Dyes

Dye	**Voc (V)**	***Jsc* (mA/cm^2)**	**Vmp (V)**	***Jmp*** **(mA/cm^2)**	**FF**	**η (%)**	**Sensitization Time**
SZD-1	0.449	1.390	0.326	1.247	0.651	0.407	3 hrs.
SZD-2	0.449	2.005	0.306	1.644	0.559	0.503	3 hrs.
SZD-3	0.510	4.760	0.306	3.948	0.497	1.208	3 hrs.
SZD-4	0.326	0.304	0.408	0.374	0.649	0.099	3 hrs.
SMA-06	0.422	0.481	0.312	0.420	0.645	0.131	3 hrs.
PT4N	0.459	0.466	0.336	0.402	0.633	0.135	3 hrs.

Chapter Summary

This chapter summarizes the results obtained by optical and photochemical properties of fabricated device as well as the analysis related to dyes used in this study. These studies highlight the performance of these dyes along with their respective functions and properties attributing in the enhancement of DSSC performance. The comparison presented in this study emphasize on the importance of photoanode metal oxide material and its affinity of dye being sensitized on it. This interaction dictates the final outcome of the device by promoting flaws and qualities of the used material.

References

[1] C. M. Pelicano, N. J. Rapadas, and E. Magdaluyo, “X-ray peak profile analysis of zinc oxide nanoparticles formed by simple precipitation method,” *AIP Conf. Proc.*, vol. 1901, no. 1, p. 020016, Dec. 2017.

[2] A. H. Javed *et al.*, “Effect of ZnO nanostructures on the performance of dye sensitized solar cells,” *Sol. Energy*, vol. 230, pp. 492–500, Dec. 2021.

[3] Y. Sun, A. C. Onicha, M. Myahkostupov, and F. N. Castellano, “Viable alternative to N719 for dye-sensitized solar cells,” *ACS Appl. Mater. Interfaces*, vol. 2, no. 7, pp. 2039–2045, Jul. 2010.

[4] C.-Y. Chen, S.-J. Wu, C.-G. Wu, J.-G. Chen, and K.-C. Ho, “A Ruthenium Complex with Superhigh Light-Harvesting Capacity for Dye-Sensitized Solar Cells,” *Angew. Chemie*, vol. 118, no. 35, pp. 5954–5957, Sep. 2006.

[5] G. Shabir *et al.*, “The Development of Highly Fluorescent Hemicyanine and Dicyanoisophorone Dyes for Applications in Dye - Sensitized Solar,” *J. Fluoresc.*, pp. 799–815, 2022.

[6] J. E. Rossini, A. S. Huss, J. N. Bohnsack, D. A. Blank, K. R. Mann, and W. L. Gladfelter, “Binding and static quenching behavior of a terthiophene carboxylate on monodispersed zinc oxide nanocrystals,” *J. Phys. Chem. C*, vol. 115, no. 1, pp. 11–17, Jan. 2011.

[7] K. Kilså, E. I. Mayo, B. S. Brunschwig, H. B. Gray, N. S. Lewis, and J. R. Winkler, “Anchoring group and auxiliary ligand effects on the binding of ruthenium complexes to nanocrystalline TiO2 photoelectrodes,” *J. Phys. Chem. B*, vol. 108, no. 40, pp. 15640–15651, Oct. 2004.

[8] S. Z. Topal, K. Ertekin, D. Topkaya, S. Alp, and B. Yenigul, “Emission based oxygen sensing approach with tris(2,2′-bipyridyl) ruthenium(II)chloride in green chemistry reagents: Room temperature ionic liquids,” *Microchim. Acta*, vol. 161, no. 1–2, pp. 209–216, 2008.

[9] K. Avhad *et al.*, “Rhodanine-3-acetic acid containing D-π-A push-pull chromophores: Effect of methoxy group on the performance of dye-sensitized solar cells,” *Org. Electron.*, vol. 65, pp. 386–393, Feb. 2019.

[10] W. C. Chang, L. Y. Lin, and W. C. Yu, “Bifunctional Zinc Oxide Nanoburger

Aggregates as the Dye-Adsorption and Light-Scattering Layer for Dye-Sensitized Solar Cells," *Electrochim. Acta*, vol. 169, pp. 456–461, Jul. 2015.

[11] W. C. Chang, L. Y. Lin, and W. C. Yu, "Dual-functional zinc oxide aggregates with reaction time-dependent morphology as the dye-adsorption layer for dye-sensitized solar cells," *J. Electroanal. Chem.*, vol. 757, pp. 159–166, Nov. 2015.

[12] K. Subramaniam, A. B. Athanas, and S. Kalaiyar, "Dual anchored Ruthenium(II) sensitizer containing 4-Nitro-phenylenediamine Schiff base ligand for dye sensitized solar cell application," *Inorg. Chem. Commun.*, vol. 104, pp. 88–92, Jun. 2019.

[13] A. B. Athanas, K. Subramaniam, S. Thangaraj, and S. Kalaiyar, "Amine functionalized homoleptic ruthenium(II) sensitizer for dye-sensitized solar cells: A combined effect of ancillary ligands and co-sensitization," *Int. J. Energy Res.*, vol. 44, no. 3, pp. 1899–1908, Mar. 2020.

[14] R. Vittal and K. C. Ho, "Zinc oxide based dye-sensitized solar cells: A review," *Renew. Sustain. Energy Rev.*, vol. 70, pp. 920–935, Apr. 2017.

[15] C. P. Lee *et al.*, "Synthesis of hexagonal ZnO clubs with opposite faces of unequal dimensions for the photoanode of dye-sensitized solar cells," *Phys. Chem. Chem. Phys.*, vol. 13, no. 47, pp. 20999–21008, Dec. 2011.

[16] W. C. Chang, T. C. Tseng, W. C. Yu, Y. Y. Lan, and M. Der Ger, "Graphene/ZnO nanoparticle composite photoelectrodes for dye-sensitized solar cells with enhanced photovoltaic performance," *J. Nanosci. Nanotechnol.*, vol. 16, no. 9, pp. 9160–9165, Sep. 2016.

[17] M. K. Nazeeruddin, E. Baranoff, and M. Grätzel, "Dye-sensitized solar cells: A brief overview," *Sol. Energy*, vol. 85, no. 6, pp. 1172–1178, Jun. 2011.

[18] M. E. Yeoh and K. Y. Chan, "Recent advances in photo-anode for dye-sensitized solar cells: a review," *Int. J. Energy Res.*, vol. 41, no. 15, pp. 2446–2467, Dec. 2017.

[19] T. Marinado *et al.*, "Rhodanine dyes for dye -sensitized solar cells : spectroscopy , energy levels and photovoltaic performance," *Phys. Chem. Chem. Phys.*, vol. 11, no. 1, pp. 133–141, Dec. 2008.

[20] S. S. Rakhunde, K. M. Gadave, D. R. Shinde, and P. K. Bhujbal, "Engineered

Science Effect of Dye Absorption Time on the Performance of a Novel 2-HNDBA Sensitized ZnO Photo anode Based Dye-Sensitized Solar Cell," *Eng. Sci*, vol. 12, pp. 117–124, 2020.

[21] G. Li, L. Sheng, T. Li, J. Hu, P. Li, and K. Wang, "Engineering flexible dye-sensitized solar cells for portable electronics," *Sol. Energy*, vol. 177, pp. 80–98, Jan. 2019.

[22] L. Lu, R. Li, K. Fan, and T. Peng, "Effects of annealing conditions on the photoelectrochemical properties of dye-sensitized solar cells made with ZnO nanoparticles," *Sol. Energy*, vol. 84, no. 5, pp. 844–853, May 2010.

[23] C. Y. Jiang, X. W. Sun, G. Q. Lo, D. L. Kwong, and J. X. Wang, "Improved dye-sensitized solar cells with a ZnO-nanoflower photoanode," *Appl. Phys. Lett.*, vol. 90, no. 26, p. 263501, Jun. 2007.

Chapter 6

Conclusions and Recommendations

6.1 Introduction

This chapter presents Conclusion of the obtained results and discussions presented in the previous chapter and recommend future work related to this study.

6.2 Conclusions

Ruthenium dyes are widely used dyes in DSSCs because of their optical properties and complex structure. Organic dyes are also being used DSSCs as an alternative to ruthenium dyes. This study shows a comparative analysis of ruthenium and organic dyes. Although ruthenium dyes have shown better electrical and optical properties, ZnO-based Ru-complex sensitized DSSCs are less stable because of their lower electron transfer kinetics and acidic nature of Ru-dyes. The recombination because of trap states and grain boundaries increases the losses of the device already bearing interfaces recombination of electrons. SZD-1, SZD-2, and SZD-4 are showing efficiency of 0.40%, 0.50%, and 0.09%, respectively. The low efficiency is the consequence of the Zn2+/dye molecule insulating layer on the ZnO surface, less stability of anchoring group, water-induced desoption of the dye molecule, and bleaching of photoanode. SZD-3 has shown an efficiency of 1.02% because of the stable nature of the Nitro group on the surface of the ZnO photoanode. Organic dyes have shown comparable results despite their simpler structure and lesser optical intensities. Due to their smaller molecular structure, aggregation of organic dye molecules decreased the output of the device and the light-harvesting property of dye. In comparison with SZD-3, SMA06 and PT4N have shown an efficiency of 10% and 11%, respectively. Some efforts in the structural tuning and development of the sensitizers along with the selection of an appropriate anchoring group can enhance the overall outcome of the device.

6.2 Recommendations

Following are the recommendations for future work on this topic:

- Titanium based DSSC fabrication using Ruthenium based these sensitizer
- Titanium based DSSC fabrication using rhodamine and dicyanoisophorone sensitizer
- Doping of ZnO nanorice for enhanced performance in DSSC
- ZnO nanorice and Titanium based DSSC comparison with same sensitizers

Chapter Summary

This chapter concludes the drawback and improvements of DSSCs fabricated by using Ruthenium (SZD-1, SZD-2, SZD-3 and SZD-4) and organic sensitizer (SMA-06 and PT4N). It also highlights the drawbacks of ZnO photoanode and the downside of Ruthenium sensitizer usage in DSSC. Also, it recommends the future work related to this research to better evaluate the performance of dyes by using different photoanodes.